PHOTOSENSITIZED DEGRADATION OF CHLOROTHALONIL AND CHLORPYRIFOS IN THE PRESENCE OF ARCTIC DERIVED DISSOLVED ORGANIC MATTER

By

Ginna Quesada, B.S.

A Thesis submitted in partial fulfillment of the requirements

for the degree of

Master of Science

in

Chemistry

University of Alaska Fairbanks

May 2021

Approved:

Dr. Jennifer Guerard, Committee Chair
Dr. Brian Rasley, Committee Co-Chair
Dr. Thomas Green, Committee Member
Dr. Tom Green, Chair
Department of Chemistry and Biochemistry
Dr. Kinchel Doerner, Dean
College of Natural Science and Mathematics
Dr. Richard Collins, Director of the Graduate School

ABSTRACT

Pesticides used at mid latitudes can accumulate in Arctic environments. Two commonly detected pesticides in Arctic lakes are chlorothalonil and chlorpyrifos. In surface waters, photolysis can play an important role in the attenuation of contaminants. The chemical characteristics of dissolved organic matter (DOM) can further alter the extent of photolytic degradation of pollutants. To determine the relative effect of natural Arctic lake water and its DOM on the photolysis of chlorpyrifos, experiments were conducted under natural Arctic irradiation and under artificial irradiation. Similarly, the effect of Arctic DOM was investigated for chlorothalonil under artificial irradiation. The fulvic acid (FA) fraction of DOM was isolated from Fog 1 and from Toolik Lake in May and July. Lake waters significantly enhanced the photodegradation of chlorpyrifos under natural light by up to an order of magnitude. FA's significantly increased the degradation of chlorpyrifos (>2x) and chlorothalonil (>100x) under artificial irradiation relative to 18 MΩ-cm Water. Toolik Lake FA isolated in May, significantly enhanced the photolysis of both contaminants relative to the isolate collected in July. In the presence of iron, a lower ratio of carbohydrates and peptides to aromatics in the FA's was associated with faster degradation for chlorothalonil.

TABLE OF CONTENTS

LIST OF FIGURES

LIST OF TABLES

LIST OF APPENDICES

DEDICATION

To my parents Jeannette Quesada and Carlos Lizano

ACKNOWLEDGEMENTS

This research was entirely funded by the National Science Foundation and could not have been accomplished without their financial contributions. I would like to thank Jennifer Guerard, my thesis advisor, for her patience and guidance throughout this process. Her support has been essential for the completion of this project and her enthusiasm for the work provided me with consistent motivation. Thanks to Jeffrey-Perala Dewey, Jill Kerrigan, and Lauren O'Connor for all your help in the field and with overcoming laboratory hurdles. All of you have provided great support in this research. I am very grateful to Dr. Rasley for all his support with instrumentation and for helping me deepen my grasp of chemical principles. A special thanks to Dr. Green for addressing all my curiosities. I would also like to acknowledge Clyde Barlow and Andrew Brabban whose inspiration has had a lasting effect on my academic and professional pursuits. Without their influence and sincere encouragement, I would have never dreamed of getting this far in the field of science. My gratitude also extends to the Toolik Field Station for providing accommodations for the field work required for this research.

CHAPTER 1. INTRODUCTION

Organochlorine pesticides have been widely used for agricultural and industrial applications since the 1940's [1]. Since then, the Stockholm Convention has identified several as persistent organic pollutants in the environment and there have been ongoing efforts to research the fate and transport of emerging organo-halogen contaminants. Two current use pesticides (CUPs) that are of toxicological concern for aquatic organisms and that have been recently detected in the Arctic are chlorpyrifos and chlorothalonil (Fig 1.1) [2-8].

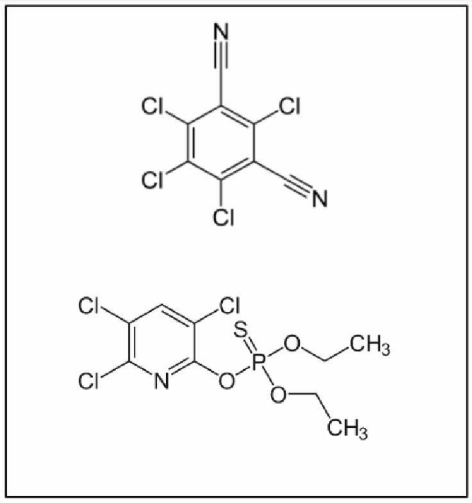

Figure 1.1. Chemical structures of contaminants. Chlorothalonil (top) and chlorpyrifos (bottom).

Chlorpyrifos is an insecticide used predominately to deter flies in feedlots and soil and foliage pests [9]. Chlorpyrifos affects the function of an insect's nervous system by disrupting nicotine acetylcholinesterase activity [10]. Based on the latest survey in the United States 5-9 million pounds of chlorpyrifos were used annually, between 2007-2012 across all market sectors, ranking as the most heavily used organophosphate insecticide during those years [11]. Chlorothalonil is a broad-spectrum fungicide that functions primarily by depleting glutathione reserves [12]. In the

agricultural market sector 6-16 million pounds of chlorothalonil were used in 2012 ranking as the 10^{th} most used pesticide in the nation [11].

Chlorpyrifos and chlorothalonil are not produced or sourced in the Arctic but their detection in air samples indicates atmospheric long-range transport into northern latitudes [13]. Air-mass back trajectories indicate that the main sources of contamination originate from mid latitudes in Asia and North America [14]. As both pesticides have henry's law constants within the range of 10^{-6} – 10^{-7} atm m^{-3} mole at 25°C, they are considered semi-volatile organic compounds whose proposed transport mechanism is through sorption onto aerosol particles [15-17]. Currently, there have been multiple studies assessing the degradation of these pesticides in natural waters at mid latitudes and multiple studies on the accumulation of these pesticides in the Arctic. However, there are no studies assessing the degradation and fate of these pesticides in the Arctic.

1.1. ACCUMULATION IN THE ARCTIC

1.1.1. Concentrations in Arctic Environmental Media

Chlorpyrifos concentrations reported in the Arctic between the years of 2007 to 2015 in air, seawater/sea-ice meltwater, and ice ranged from 1.1-6.8 pg/m^3, 0.74-14.1 pg/L, and 5.2-14.4 pg/L respectively [18]. In Arctic snow, 4.8 ±1.3 pg/L of chlorpyrifos have been reported, and the highest concentration of chlorpyrifos that has been determined is 1600 pg/L in Arctic lake water [19].

Chlorothalonil concentrations reported in the Arctic between the years of 2007 to 2015 in air ranged from 0.1-2.1pg/m^3 and an average of 322 pg/L were found in seawater/sea-ice meltwater [18]. Chlorothalonil concentrations in snow have been reported as 537 ± 563.7 pg/L and the greatest concentration reported for Arctic lakes has been 2800 pg/L [19-20]. In the last 10 years it has been approximated that the Arctic is losing its ice cover at the rate of -10.1-10.7% per decade [21].

Consequentially, as the Arctic continues to warm, CUP's that are currently sequestered in ice will be further released into alternate environmental media. Melt ponds from sea ice are predicted to discharge 4% of chlorpyrifos and chlorothalonil loads annually into ocean waters, increasing their availability to influence Arctic ecosystems [22].

1.1.2. Concentrations in biota

During the 2007-2010 period, chlorpyrifos and chlorothalonil concentrations in three marine food chains located in the Canadian Arctic Archipelago were quantified. Chlorpyrifos was detected in plankton, char, capelin, and in polar bear fat. Chlorothalonil was detected in ice-algae, plankton, polar cod, Arctic cod, char, capelin, and polar bear fat. The greatest concentrations of chlorpyrifos were found in Plankton at 1.1 ng/g of lipid weight (lw). The greatest concentrations of chlorothalonil were reported for capelin as 1.4 ng/g lw. Chlorothalonil and chlorpyrifos were both found to bioaccumulate (calculated as the ratio of the arithmetic mean concentrations of the contaminant in the organism to the seawater concentrations) in plankton, *boreogadus saida*, char, and capelin. Both pesticides exhibited their greatest bioaccumulation factors (log BAF- calculated as the log of the ratio of the arithmetic mean concentrations of the contaminant in the organism to the seawater concentrations) in plankton ranging from 6.9 L/kg – 7.4 L/kg lipid weight. Both pesticides were also found to bio-magnify in mammals and fish. For chlorpyrifos and chlorothalonil the greatest biomagnification factors (BMF- calculated as the ratio of the arithmetic mean concentrations of the contaminant in the organism to their diet's concentrations) were found in bears as 0.9 ± 0.27 and 3.7 ± 0.63 and in capelin as 0.53 ± 0.36 and 2.7 ± 0.03 respectively [23]. Chlorpyrifos and chlorothalonil have also been detected in terrestrial Arctic biota. In a study conducted in the Bathurst region of the Canadian Arctic chlorpyrifos was found to bioconcentrate

most in mushrooms (0.85 ng/g lw) and in caribou muscle (0.4 ng/g lw). Chlorothalonil's greatest concentrations were found in moss (0.69 ng/g lw) and in wolf muscle (0.44 ng/g lw) [24].

1.2 SUB-LETHAL TOXICITY

1.2.1. Neurotoxicity of chlorpyrifos

Organophosphate toxicity is generally attributed to the inhibition of acetylcholinesterase through the binding of the phosphate moiety to the serine binding site of the enzyme. This inhibition results in an over accumulation of acetylcholine in the synaptic cleft which leads to the excessive depolarization of the post-synaptic neuron. The previous results in seizure activity and necrosis [25]. Fathead Minnows placed in an aqueous environment containing chlorpyrifos at a concentration of 0.12 µg/L for 200 days experienced 10% brain acetylcholinesterase inhibition and reduced growth in second-generation fish [26]. Coho salmon analyzed for acetylcholinesterase activity, after 96 hours of exposure to chlorpyrifos (0.6 µg/L), had about a 5% and 4% decrease in enzymatic activity in the brain and muscle tissue respectively [27]. At a concentration of 35 µg/L of chlorpyrifos zebrafish lost up to 71% of muscle acetylcholinesterase activity and had an increased number of anti-predator immobilization responses [8].

Chlorpyrifos toxicity at concentrations below the induction of acetylcholinesterase inhibition have been found to be associated with the modification of neurotrophic factors and increased levels of NMDA receptors and extracellular glutamate [28]. Chlorpyrifos has also been shown to disrupt normal patterns of neuronal connectivity through the inhibition of long axonal growth ([chlorpyrifos] = 35 ng/L) and the promotion of dendritic branching ([chlorpyrifos] = 0.35 mg/L) in embryonic rat sympathetic neurons [29]. The literature suggests that chlorpyrifos can alter the complex organization of the nervous system to a potentially deleterious extent.

In various studies, conducted in vivo, chlorpyrifos has also been shown to induce various behavioral changes that occur below the induction of acetylcholinesterase inhibition. Weanling rats injected with 3 mg/kg of chlorpyrifos every 4 days showed impaired spatial learning [30]. Coho salmon exposed to 0.63 μg/L of chlorpyrifos for seven days had decreased amplitudes of bulbar and epithelial responses to taurocholic acid and L-serine odorants. The reduced olfactory function could potentially pose a risk for salmon migration and behaviors that are crucial for survival [27]. The concentrations at which the behavioral changes in Coho salmon have occurred are two orders of magnitude greater than the highest reported concentration for chlorpyrifos in the Arctic (1.6 ng/L). The previous suggests that similar effects may be occurring for aquatic species in Arctic environments and further investigations are required.

The neurotoxic effects of chlorpyrifos can be altered when combined with other neurotoxic agents such as glucocorticoids. In one study the combined effects of dexamethasone (dose: 100 nM) and chlorpyrifos (dose: 10 or 50 μM) were examined in PC12 cells undergoing neurodifferentiation. Both chlorpyrifos and dexamethasone independently caused a concentration dependent decline in the number of PC12 cells and induced cellular hypertrophy. The combined exposure to the corticosteroid and high concentrations of the pesticide resulted in additive effects [31]. Increased levels of cortisol in the plasma of cold-water fish such as the brook trout have been reported as a consequence of elevated temperatures [32]. As the climate in the Arctic continues to change, the combined exposure to chlorpyrifos and increased levels of glucocorticoids could also result in complex alterations to Arctic ecosystems.

Chlorpyrifos toxicity has been found to occur at concentrations as low as 35 ng/L in vitro but a common concern with in vitro experiments is that they require greater concentrations than in vivo systems to cause toxicity and many of the toxic mechanisms studied in vitro have yet to be tested

in vivo [29, 33]. The absence of these studies entails a deficit in the ability to accurately predict the potential neurotoxic risk on ecosystems in the Arctic.

1.2.2. Immunotoxicity of chlorothalonil

The primary toxic mechanism of chlorothalonil occurs through the nucleophilic aromatic substitution of a chlorine atom by deprotonated glutathione (GSH) [12]. The formation of the 4-glutathion-S-yl conjugate of chlorothalonil limits the intracellular concentration of GSH. Consequently, the scavenging of reactive oxygen species by glutathione peroxidases, that require the concomitant oxidation of GSH, is impaired. Syrian hamster embryo cells treated with 0.5 μg/mL of chlorothalonil had a 35% reduction in GSH/mg protein after 144 hours of exposure. Owing to its ability to cause oxidative stress, it has been found to serve as a promoter for tumor formation in hamster embryos and cause carcinogenic effects on the kidney and stomach [34].

Melanomacrophages and granulocytes are leukocytes that help the immune system respond to parasites. Tadpole liver melanomacrophages and granulocytes were counted post exposure to 0.5 μg/L of chlorothalonil and a 2-fold decrease in the number of leukocytes was observed. Furthermore, corticosterone concentrations in the tadpoles more than doubled post exposure to 16.4 μg/L of chlorothalonil [6]. NADPH oxidase is essential for macrophages to mediate non-specific immunity via the production of reactive oxygen species. At the exposure levels of 10.6 μg/L and 53.2 μg/L of chlorothalonil superoxide anion production in striped bass macrophages decreased by approximately 40% and 90% respectively, indicating a substantial suppression of NADPH oxidase activity [2]. Chlorothalonil has also been found to cause DNA damage to leukocytes. When exposed to 2.65 mg/L of chlorothalonil, 90% of human peripheral blood lymphocytes had DNA damage and a 25% loss of cell viability was observed [35].

Hemolytic anemia is not an immune system disorder; however, the premature destruction of red blood cells can impair the functioning of the immune system. Plasma free heme can disrupt macrophage phagocytosis and microbial defense and it can suppress effector T-Cell response by inhibiting dendritic cell maturation [36]. At low oxygen concentrations (5 mg/L) *Salmo gairdneri* exposed to 2 µg/L of chlorothalonil for 24 days experienced a 33.7% decrease in hematocrits leading to acute hemolytic anemia. No detrimental effects on hematocrits were observed at the low oxygen concentrations without chlorothalonil exposure [3].

Chlorothalonil toxicity has been found to occur at concentrations as low as 2 µg/L during in vivo studies and 0.5 µg/L in in vitro studies. These concentrations are two to three orders of magnitude greater than the greatest reported concentration (2.8 ng/L) found in arctic environments. Based on current data it does not appear that chlorothalonil is posing a threat to Arctic ecosystems. Nevertheless, this pesticides' ability to bioaccumulate may cause adverse effects when coupled to environmental changes that result from global warming. With the decline in global dissolved oxygen concentrations the threat of chlorothalonil to aquatic arctic ecosystems could potentially increase. In the past five decades the Arctic has contributed to a 7.6 +/- 3.1% loss of total global oxygen concentrations. As temperatures continue to rise in Arctic environments oxygen concentrations will continue to drop and may play an increasingly crucial role in determining the risk that chlorothalonil poses to aquatic ecosystems [37].

1.3. CHLORPYRIFOS ENVIRONMENTAL ATTENUATION MECHANISMS

1.3.1. Microbial Degradation

Chlorpyrifos is primarily attenuated in the environment through microbial degradation whereby at a concentration of 250 mg/L the Enterobacter strain B-14 degrades 100% of chlorpyrifos in three days [38]. The bacterial strain C2A1 was reported to degrade 82% of chlorpyrifos at a starting

concentration of 50 mg/L in 5 days [39]. Although microbial degradation is effective for the attenuation of chlorpyrifos, the formation of its recalcitrant metabolite 3,5,6-trichloro-2-pyridinol (TCP) can reduce the efficacy of microbial degradation in natural waters [40]. Additionally, at lower temperatures microbial degradation for chlorpyrifos has been found to become less efficient [15].

1.3.2. Hydrolysis

Chlorpyrifos hydrolysis has been found to follow a pseudo-first order rate kinetics model and has reported half-lives ranging from 75 hours to 35.3 days at pH 6 - 6.9. Under alkaline conditions at pH 8 reported half-lives range from 64 hours to 22.8 days. Despite the large discrepancy in the literature regarding the hydrolysis half-lives of chlorpyrifos, it has been shown that chlorpyrifos is more susceptible to hydrolysis under basic conditions. Additionally, natural water has been found to have an enhancement effect on the rate of chlorpyrifos hydrolysis. In both pond and canal water hydrolysis rates increased 16-fold, indicating that metal ions have a catalytic effect on the hydrolysis of chlorpyrifos [41-42]. Alternatively, waters with high concentrations of dissolved organic matter (34 mg/L) have been found to decrease the hydrolysis rate of chlorpyrifos by 32% [43]. Chlorpyrifos hydrolysis has also been found to decrease at lower temperatures with up to a 3.5-fold rate retardation for each 10°C drop in temperature [41-42]. The main chlorpyrifos hydrolysis products that have been reported are 3,5,6-trichloro-2-pyrinidol, o-ethyl o-hydrogen o-(3,5,6 trichloro-2-pyridyl) phosphorothioate, o-dihydrogen o-(3,5,6 trichloro-2-pyridyl) phosphorothioate [42].

1.3.3. Aqueous Photolysis

Photolysis has been found to play a greater role than hydrolysis in the attenuation of chlorpyrifos in aqueous systems. At circumneutral and in acidic pH environments photolysis has been found to have a 1.3 to 3.8 times greater effect on the degradation rate of chlorpyrifos as opposed to

hydrolysis [44]. Although photolysis plays a crucial role in the attenuation of chlorpyrifos, inconsistent trends have been observed for the catalytic effect of natural waters on its photodegradation. Most studies have found that there is no statistically significant difference between photodegradation rates in deionized water compared with natural waters [45-47]. However, a study using prairie pothole waters did find photodegradation rate enhancement in natural water versus borate buffered deionized water at a basic pH [48]. The difference between findings could be attributed to the fact that the former studies all contained a co-solvent for the dissolution of chlorpyrifos and the latter did not. Co-solvents such as acetonitrile or methanol can distort the concentrations of reactive species and thereby alter the observed results [49]. In natural waters photolysis half-life values under artificial light range from 6 minutes to 60 hours. In deionized water under artificial light values have ranged from 5 minutes to 93.9 hours [45-47]. Furthermore, the calculated environmental half-life at 40°N in river water is almost 23 times greater than in deionized water [50]. Direct photolysis has been determined to account for about 50% of chlorpyrifos degradation in natural waters. Singlet oxygen, hydroxyl radicals, and carbonate radicals, listed in order of decreasing reactivity, are the main reactive species that contribute to the photodegradation of chlorpyrifos [48]. The only photo products that have been identified in water are 3,5,6-trichloro-2-pyrinidol, chlorpyrifos oxon, and o-ethyl o-hydrogen o-(3,5,6 trichloro-2-pyridyl) phosphorothioate [42, 46-47]. No photoproducts resulting from the further decomposition of TCP have been identified in the literature despite speculations that poly-hydroxy-pyridines and quinoid type products could be formed from the further photodegradation of TCP [44, 51-52]. Additionally, Fenton-type reactions have been found to have a catalytic effect on the photolysis of chlorpyrifos. Chlorpyrifos' half-life was reduced four-fold in the presence of ferric chloride and hydrogen peroxide [46].

1.4. CHLOROTHALONIL ENVIRONMENTAL ATTENUATION MECHANISMS

1.4.1. Microbial Degradation

Chlorothalonil at a starting concentration of 1500 mg/L has been found to degrade 53.3% in 14 days in a bacterial mixed culture obtained from agricultural soils [53]. The combined presence of both chlorpyrifos and chlorothalonil has been reported to reduce the efficacy of microbial degradation in natural systems [54]. Lastly, at lower temperatures microbial degradation has been found to become less efficient [55].

1.4.2. Hydrolysis

Chlorothalonil hydrolysis has been determined to be both negligible and substantial, with a half-life of 17 days below pH 9. Under basic (pH > 9) aqueous conditions chlorothalonil has been reported to have a pseudo-first order rate of degradation with a half-life ranging from 2.1 days to 38.1 days [56-57]. The main hydrolysis products identified for chlorothalonil, under dark conditions, are 3-cyano-2,4,5,6-tetrachlorobenzamide, 4-hydroxy-2,5,6-trichloroisophthalonitrile, and trichloro-1,3-dicyanobenzene [56, 58].

1.4.3. Aqueous Photolysis

Chlorothalonil has been found to degrade readily in natural water through direct photolytic pathways and its rate of degradation has been reported to increase in the presence of photosensitizers such as dissolved organic matter [59-61]. In deionized water under artificial solar irradiation, reported half-lives for chlorothalonil have ranged from 6.5 hours to 36.86 hours [59-62]. Under aerobic conditions the direct degradation mechanism has been reported to occur predominantly by the reaction between triplet excited state chlorothalonil and water to form 4-hydroxy-chlorothalonil and unstable hydroperoxyl radicals [62]. In the presence of natural whole water under artificial light, reported half-lives range from 0.71 hours to less than 24 hours [56, 59,

[61]. Reported half-lives for photolysis experiments conducted in the presence of fulvic acids (~5 mg/L) range from 3.1 to 4.3 hours [60, 61]. Additionally, an increase in the concentrations of dissolved organic matter has been found to further enhance the photodegradation of chlorothalonil. A five-fold increase in the concentration of fulvic acids has been reported to decrease the half-life of chlorothalonil by almost 40% [61]. The two main degradation pathways that have been most recently described in the literature are through the energy transfer reaction from triplet excited state humic substances onto chlorothalonil and through electron and hydrogen donating properties of triplet excited state humic substances [60]. Photoproducts that have been identified in the presence of electron donors are trichloro-1,3-dicyanobenzene, chloro-1,3-dicyanobenzene, dichloro-1,3-dicyanobenzene, 4-hydroxy-chlorothalonil, 2-hydroxy-chlorothalonil, 3-cyano-2,4,5,6-tetrachlorobenzamide, and benzamide [56, 60-62]. Oxygen has been reported to have an inhibiting effect on the rates of photolysis. Such that the triplet decay of chlorothalonil was found to be governed by reactivity with oxygen [60, 62]. Photodegradation enhancement in oxygenated media was concluded to be a consequence of the electron and hydrogen donating capacity of the humic substances used whereby the Elliot fulvic acids and carbonaceous humic acids had the greatest enhancement effect on degradation. Reactions with TMP were found to indicate that triplet excited humic substances induced the triplet excited state of chlorothalonil [60]. Lastly, Fenton-type reactions have been found to have a catalytic effect on the photolysis of chlorothalonil. Chlorothalonil's half-life decreased twenty-seven-fold in the presence of ferric chloride and hydrogen peroxide [59].

1.5. IMPLICATIONS FOR RESEARCH

As a result of warming temperatures in Arctic environments there is an ongoing increase in primary productivity, microbial activity, and permafrost melt which can lead to an increase in dissolved

organic carbon (DOC) in aqueous systems [63-64]. Dissolved organic carbon is sourced from plant matter and cellular components such as lignin, cellulose, amino acids, peptides and the decomposition products of these larger metabolites. In aquatic systems DOM can act as a photosensitizer, changing the rate of photolytic reactions, as well as influencing the composition of photo transformation products [65]. Additionally, the chemical composition of DOM influences its reactivity with pollutants. Studies have shown that DOM characterized by having more aromatic moieties tends to promote the production of reactive oxygen species and hydroxyl radicals. Alternatively, DOM with less aromaticity tends to become excited into its triplet state and oxidize contaminants directly [66-67]. Variability in the chemical composition of dissolved organic matter is dependent on source materials and has been shown to have an effect on the photo reactivity of organic pollutants [65, 67]. For example, DOM with greater aromaticity has been found to have a greater electron donating capacity than less aromatic DOM [68]. Additionally, DOM sourced from different locations can alter the steady state concentrations of reactive intermediates [48]. Arctic derived DOM forms unique hydrolysis products and possess a significantly different functional group composition and reactivity than DOM sourced from other environments [69-70]. Furthermore, iron is one of the main reducing species in Arctic lakes and could potentially have an accelerating effect on the indirect photodegradation of these two pesticides via the production of reactive oxygen species [71].

Despite the unique characteristics of Arctic DOM and its aqueous environment, a study has not yet been done on the photochemical fate and transformation of chlorpyrifos and chlorothalonil in Arctic lacustrine systems. With lower temperatures in Arctic environments the microbial and hydrolytic degradation rates of these contaminants are inevitably reduced which imparts a greater

burden on photolytic processes to attenuate contaminants. As a result of increasing deposition of both DOM and contaminants into Arctic waters, coupled with the seasonal reduction of hydrolysis and biodegradation efficiency, photolysis will become increasingly important for the attenuation of these compounds. Currently, there have been only theoretical calculations of the half-life for chlorpyrifos in the Arctic with an estimated half-life of 218 days in Arctic waters [19]. A half-life of 218 days would be approximately 57 times greater than the greatest reported half-life in deionized water, entailing a degradation rate that is more than twice as slow as the environmental photolysis rate calculated at 40°N in river water [48, 50]. The previous half-life was calculated using the software EPIWIN which has been reported to typically underestimate the half-lives of potential persistent organic pollutants, so it is crucial to obtain empirical values [72].

This research aims to investigate the effect of natural Arctic waters on the photodegradation rates of chlorpyrifos and chlorothalonil. The objective of this research is to determine the photodegradation kinetics of chlorpyrifos and chlorothalonil in the presence of fulvic acids sourced from Arctic Lakes, with and without the addition of iron, relative to 18 MΩ-cm water and DOM sourced from Pony Lake, Antarctica and Suwannee River, Georgia. It is hypothesized that both the presence of iron and DOM sourced from Arctic lakes will enhance the photochemical degradation of both contaminants. Relationships between the chemical composition of the various DOM extracts and the rates of degradation of the two contaminants are explored in order to attain insight on the possible degradation pathways. Furthermore, this research examines the effect of whole waters on the photodegradation of chlorpyrifos under natural solar irradiation at 69°N.

2. METHODS

2.1. CHEMICALS AND STANDARD SOLUTIONS

Chlorothalonil (purity ≥98%) and chlorpyrifos (purity ≥98%) used for standard preparation were purchased from Sigma Aldrich (St. Louis, MO, USA). HPLC grade acetonitrile and methanol were obtained from EMD Millipore Corporation (Darmstadt, Germany). Glacial acetic acid (≥99%) for the preparation of HPLC eluent mixtures was obtained from AlfaAesar (Wardhill, MA). For photodegradation experiments pH adjustments were made using anhydrous sodium hydroxide (purity 97%) purchased from Sigma Aldrich (St. Louis, MO, USA) and hydrochloric acid (≥36.5%) obtained from Macron Fine Chemicals™ (Radnor, PA, USA). Ferric chloride hexahydrate anhydrous ($FeCl_3$) used for fenton type experiments was acquired from Arcos Organics (Morris, NJ). Para-nitroanisole (purity 99%) used for actinometry experiments was obtained from ACROS Organics™ (UK). Chlorpyrifos (purity ≥99%) used for quality control standards was purchased from Restek (Bellefonte, PA). Suwannee River and Pony Lake fulvic acid material was obtained from the International Humic Substances Society (IHSS). All diluent water used was type I 18.2 MΩ-cm water purified with a Milli-Q® water system, hereinafter simply referred to as 18.2 MΩ-cm water. Chlorpyrifos stock solutions (600 μM) and working standard solutions (0.1-10 μM) were prepared in acetonitrile. Chlorothalonil stock solutions (1000 μM and 6 μM) were prepared in acetonitrile. Chlorothalonil working standard solutions (0.12 μM – 12 μM) were prepared daily by diluting the stock solution with unbuffered 18.2 MΩ-cm water. Working standard concentrations were determined based on the solubility of chlorpyrifos and chlorothalonil in 18.2 MΩ-cm water. For total organic carbon (TOC) analysis, potassium hydrogen phthalate (≥99%) sourced from AlfaAesar (Wardhill, MA) and Sigma Aldrich (St. Louis, MO, USA) was used. For total dissolved nitrogen analysis (TN), potassium nitrate (≥99%) sourced from

Sigma Aldrich (St. Louis, MO, USA) and Fujifilm WAKO Chemicals (Japan), was used. All glassware was washed with Citranox detergent, left to sit in an acid bath (10% HCl) for a minimum of 4 hours and was pre-combusted in a muffle furnace at 450°C for 4 hours. All solutions were prepared under red light in amber borosilicate scintillation vials with PTFE lined screw caps and stored at 4°C.

2.2. SAMPLING SITES AND COLLECTION METHODS

2.2.1. Description of Sampling Sites

Surface waters were collected from Fog 1 lake (68°67'99.52''N 149°09'41.79''W), Fog 2 lake (68°68'37.59''N 149°08'29.35''W) and the outlet of Toolik lake (68°63'83.99''N 149°59'91.21''W). These oligotrophic lakes are underlain with permafrost and surrounded by tundra shrubs, herbaceous flowering plants, sedges, lichen, and moss [73-74]. The lakes begin to freeze during late September and air temperatures begin to rise above freezing during late May [75-76]. Fog 1 lake and Fog 2 lake are hydrologically isolated lakes that derive their dissolved organic matter entirely from the surrounding terrestrial runoff and atmospheric inputs (Figure 2.1.). These lakes are representative of lakes that are exclusively contaminated via the atmospheric deposition of pollutants. Alternatively, Toolik lake is a drainage lake with an inlet that has several upstream lakes and an outlet (Figure 2.1.). Toolik lake is representative of lakes that derive their dissolved organic matter and source contaminants from the surrounding terrestrial runoff, atmospheric inputs, and connected lakes and streams.

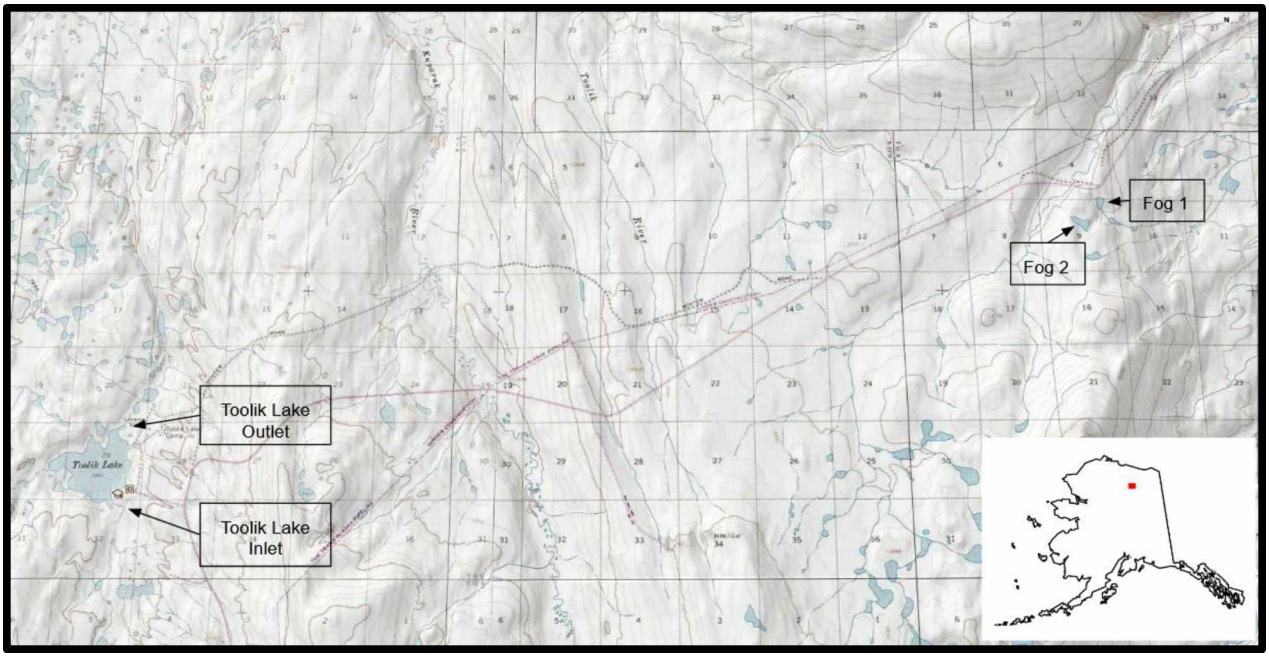

Figure 2.1. Map of sampled lakes.

2.2.2. Sampling methods

Fog 1 Lake and Fog 2 lake whole water samples were gathered on the 15th of June of 2019 and the outlet of Toolik lake was sampled on the 25th of June of 2019. Fog 1 Lake was sampled, for DOM extraction, on the 17th of June of 2019. For DOM extraction, the outlet of Toolik lake was sampled at the end of spring (5/29/19) and towards the end of summer (7/2/19). Hereinafter, the Toolik lake DOM extracts will be referred to as Toolik Early and Toolik Late DOM respectively. All plastic ware used for sample collection was washed with Citranox detergent, rinsed with a 10% HCl solution, and rinsed in triplicate with sample water. All lake water samples were collected in 10 or 20 L LDPE cubitainers (Hedwin). As water samples were collected the temperature, and specific conductivity were recorded using a YSI Professional Plus and the pH of the water was recorded using a YSI Pro2030. Toolik lake was determined to have a greater DOC concentration (5 mg/L) than both Fog lakes (3 mg/L).

Table 2.1 Lake water properties and respective experimental purpose

Lake Whole Water Source	Date Collected	Purpose for Collection	pH	Specific Conductivity (μS/cm)	Lake Temperature at time of sample collection (°C)
Toolik Outlet	6/25/19	Whole water experiment	7.28	93	12.1
Fog 1	6/15/19	Whole water experiment	7.85	100.5	8.7
Fog 2	6/15/19	Whole water experiment	7.82	97.6	8
Toolik Outlet	5/29/19	FA Extract (Early)	7.18	90	5.4
Toolik Outlet	7/2/19	FA Extract (Late)	8.34	72.3	14.4
Fog 1 DOM	6/17/19	FA Extract	7.90	102.3	9

2.3. DISSOLVED ORGANIC MATTER EXTRACTIONS

For the solid phase extraction of the fulvic acid fraction of the DOM, acidified (to pH 2 with HCl) and filtered (0.45 μM) water samples were loaded onto styrene divinyl benzene polymer (PPL) cartridges (pre-conditioned with methanol), allowed to air dry, and extracted with methanol. Extracts were placed in a rotary evaporator and reduced to an approximate volume of 10 mL and diluted with ultrapure water at a 1:10 ratio respectively. Diluted extracts were then freeze dried and stored at room temperature in borosilicate amber vials. Total non-purgeable organic carbon (TOC) and total dissolved nitrogen (TN) analysis of filtered water samples and solid phase DOM extracts were conducted using a Shimadzu 32356 TOC analyzer. Percent recoveries were calculated using the ratio of the total mass of carbon extracted, in the dissolved organic matter isolated, to the total mass of carbon that was present in the whole waters prior to extraction (Table A.2.1). For the purposes of this investigation the terms DOM and fulvic acids will be used interchangeably.

2.4. OPTICAL CHARACTERIZATION OF DOM

Absorbance and fluorescence scans were obtained on a Jobin-Yvon Aqualog-800-C (Horiba Instruments, Edison, NJ) using 1 cm quartz cuvettes (Firefly Scientific, Staten Island, NY). Absorbance scans were collected with a 0.1 second integration time at 1 nm intervals between the wavelength range of 200-800 nm. Excitation-emission matrices (EEMs) were scanned with a 0.1 second integration time on medium gain at an excitation wavelength range of 240-600 nm and at an emission wavelength range of 240-800 nm with 4-pixel resolution. EEMs of DOM extracts and 18.2 MΩ-cm water were collected in ratio mode and 18.2 MΩ-cm water blank EEMs were subtracted daily from DOM extract EEMs. EEMs were corrected for Rayleigh scattering, inner filter effect, and normalized under the water-Raman curve at an excitation wavelength of 350 nm to correct for lamp intensity variation over time. Fluorescence indexes for all fulvic acids were calculated as the ratio of fluorescence at an emission of 470:520 nm and with an excitation of 370 nm.

2.5. CHARACTERIZATION OF DOM via ^{1}H NMR SPECTROSCOPY

All DOM extracts were analyzed by solution state NMR spectroscopy. Freeze dried samples were dissolved in ultrapure water to a final concentration of ~1 mg/mL and the solutions were transferred to 5-mm 7'' Wilmad-Lab Glass NMR tubes (Vineland, NJ) for spectral analysis.

A Bruker Avance III 600-MHz NMR spectrometer was used to collect ^{1}H NMR spectra equipped with a 5-mm broadband liquids SmartPROBE^{TM} with computer controlled tuning covering ^{15}N - ^{31}P-^{19}F-^{13}C-^{1}H with ^{1}H decoupling and a Z-gradient. The solvent suppression sequence SPR-5-WATERGATE was used to suppress the water signal at ~4.9 ppm. For each spectrum 10,000 scans were acquired using a 1 μs recycle delay. The ^{1}H NMR spectra referenced a D_2O trimethylsilyl [2,2,3,3,-$^{2}H_4$]-propionate (TSP) external standard prepared at a concentration of 5.95 mM in a

sealed melting point capillary tube inserted in the NMR tube containing the DOM sample. Spectra were processed using *TopSpin* 3.6 software and structural assignments and spectral integration were done in accordance with the regions specified by Mitchell et al. 2013 [77].

2.6. PHOTOLYSIS EXPERIMENTS

Stock solutions of chlorpyrifos (22 mM) and chlorothalonil (6mM) were prepared in methanol and 450 µL and 650 µL were added respectively to 500 mL media bottles (Pyrex). The media bottles were carefully rotated by hand to increase the surface area of the bottle coated with a thin film of the solution. The methanol was left to air dry for 24 hours in a fume hood and either 300 mL (for DOM experiments) or 400 mL (for direct photolysis experiments) of pH adjusted ultrapure water was added and left to equilibrate with the pesticide thin film for an average of 18 hours. For whole water experiments 400 mL of sampled lake water was added in lieu of pH adjusted 18.2 MΩ-cm water.

For DOM experiments thin film solutions were transferred to a separate 500 mL media bottle and combined with pH adjusted DOM solutions (100 ppm) to yield a final DOM concentration of 20 ppm. Iron is one of the key reducing species in Arctic lakes and as a consequence of hydrogen peroxide formation in the presence of light and DOC. Iron can have an accelerating effect on the photodegradation of organic pollutants by increasing the concentrations of hydroxyl radicals via reactions 1-3 [71, 78].

$$\text{Fe (III)} + \text{H2O} \xrightarrow{h\nu} \text{Fe (II)} + \cdot\text{OH} + \text{H}^{+} \quad (1)$$

$$\text{Fe (II)} + \text{H}_2\text{O}_2 \leftrightarrow \text{Fe (III)} + \cdot\text{OH} + \text{OH}^{-} \quad (2)$$

$$\text{Contaminant} + \cdot\text{OH} \rightarrow \text{Products} \quad (3)$$

To investigate the influence of iron on contaminant degradation, in the presence of DOM, 20 μM of $FeCl_3$ was added in additional experiments to fulvic acid solutions. Solutions were aliquoted into 14 mm diameter, 10 cm long quartz reaction tubes sealed with Teflon lined screw caps and dark controls were aliquoted directly into HPLC amber vials. Each experiment was carried out in triplicate.

Solutions were irradiated under artificial or natural Arctic light. The ambient air temperature ranged from 12°C to 23°C in the field. In the laboratory, samples were irradiated in a Suntest CPS+ (ATLAS; Mount Prospect, Illinois) solar simulator equipped with a xenon arc lamp (500W). The temperature ranged from 17°C to 21°C in the solar simulator. The irradiation intensity was measured with a SolarLight PMA 2100 radiometer for experiments conducted under both artificial solar irradiation and under natural solar radiation. The average irradiance of experiments conducted under artificial light was recorded at each time point interval (minutes elapsed since the initial exposure of the sample to the xenon arc lamp). The average irradiance recorded under Arctic solar light was logged at 15-minute intervals for the entire duration of the experiments. Natural solar irradiance (I) was corrected for the elevation angle (EI) of the sun using equation 2.1.

$$I_{cor} = \frac{I}{\cos\theta} \tag{2.1}$$

Where θ is the zenith angle in radians as derived from $EI \times \frac{\pi}{180}$. Elevation angle values were obtained from the National Oceanic and Atmospheric Administration's Solar Calculator. The average irradiation intensity of the xenon arc lamp in the solar simulator was 6.13 mW/cm^2 and the temperature was maintained at 19°C ±2°C. The average irradiation intensity at 69°N was 1.5 mW/cm^2, with an average temperature of 17.5°C ±5.5°C. To determine the absorbed photon flux,

para-nitroanisole actinometry experiments were conducted [79]. Actinometry experiments did not contain pyridine (PYR) due to the duration of the photolysis reactions (2 to 48 hours), and they were run concurrently with whole water experiments. As a result of both the stability of emitted irradiation from the Suntest and the spatial limits of the apparatus, actinometry experiments were conducted at a separate time from all experiments conducted under solar simulated light.

Irradiated solutions of chlorpyrifos, chlorothalonil, and PNA were analyzed by reverse-phase HPLC (Agilent 1220 Infinity II) equipped with a variable wavelength detector. All separations were carried out with an Ultra C18 5 μM particle size column with an internal diameter of 4 mm and a 150 mm length (Restek, Centre County, PA). Chlorpyrifos was separated using an isocratic elution consisting of acetonitrile:0.1% acetic acid (80:20% v/v) at a flow rate of 1 mL/min, with an injection volume of 35 μL, and a column temperature of 30°C. The detection wavelength was set at 290 nm. (RT = 6.7) Chlorothalonil was separated using an isocratic elution consisting of methanol:water (70:30% v/v) at a flow rate of 1 mL/minute, with an injection volume of 50 μL, and a column temperature of 40°C. The detection wavelength was set at 233nm. (RT=5.5). PNA was separated using an isocratic elution consisting of acetontrile:water (50:50% v/v) at a flow rate of 1 mL/minute, with an injection volume of 35 μL, a column temperature of 37°C. The detection wavelength was set at 313 nm. (RT: 6.2)

Rate constants were calculated from a least-squares fit of the degradation data to the pseudo-first-order kinetics model using GraphPad Prism 8.3.0 software. Irradiance values were used to both monitor the stability of the xenon arc lamp and to calculate fluence-based pseudo-first-order rate constants (as described by Wei-Haas 2015) [80]. The recorded average irradiance per time point

(minutes elapsed since initial light exposure) or logging interval, was multiplied by the logging interval in seconds to attain the dose of energy per minute. The sum of each dose, up to the time point at which samples were removed from the light source, was used to determine the accumulated dose (J/cm^2). Time points and corresponding accumulated dose values are provided in Appendix A. The natural log of the concentration of the contaminant at any given time [C_t] vs the concentration at time zero [C_0] was plotted as a simple linear regression against the accumulated dose for the final attainment of the absolute value of the slope which yields the fluence-based rate constant in units of centimeters squared per joule.

The observed pseudo-first-order rate constants for experiments conducted solely in 18.2 MΩ-cm water is estimated to be the sum of the hydrolysis rate constant and the direct photodegradation rate constant. The observed pseudo-first-order rate constant for whole water and DOM experiments is estimated to be the sum of the hydrolysis rate constant, the direct photodegradation rate constant, and the aggregate of rate constants attributable to indirect degradation via all intermediate reactive species formed in the presence of DOM (Equation 2.2).

$$k_{obs} = k_{H2O} + k_{direct} + \sum k_{indirect} \tag{2.2}$$

For all photolysis experiments, apparent rate coefficients (k_{obs}) were corrected (k_{cor}) for aggregate light screening factors ($S_{\sum\lambda}$) over the range of 239-500 nm by equation 2.3.

$$k_{cor} = \frac{k_{obs}}{S_{\sum\lambda}} \tag{2.3}$$

Aggregate screening factors were determined by plotting wavelength specific screening factors S_λ, using equation 2.4

$$S_\lambda = \frac{1 - 10^{-\alpha_\lambda l}}{2.303\alpha_\lambda l} \tag{2.4}$$

where α_λ (cm^{-1}) is the attenuation coefficient and l (cm) is the pathlength of the quartz tubes (1 cm), by their corresponding wavelength and fitting them to a polynomial function. The determined least squares equation was integrated within the wavelength range of interest. The resulting areas were then normalized to the area anticipated if there were no light screening to obtain $S_{\sum\lambda}$. The aggregate screening factors were calculated in accordance with the method used by Miller and Chin's [81].

For the determination of the apparent quantum yields (φ_{dc}), for whole water experiments conducted under natural solar irradiation, equation 2.5 was used

$$\varphi_{dc} = \frac{k_{dc}}{k_{da}} \frac{\sum_\lambda \varepsilon_{\lambda a} L_\lambda \lambda_{Range}}{\sum_\lambda S_\lambda \varepsilon_{\lambda c} L_\lambda \lambda_{Range}} \varphi_{da} \tag{2.5}$$

where k_{dc} is the apparent rate constant for the contaminant degradation and k_{da} is the apparent rate constant for the degradation of the actinometer. Equation 2.6 was employed for the calculation of the PNA/PYR actinometer's quantum yield (φ_{da}) [82].

$$\varphi_{da} = 0.437[\text{PYR}] + 0.000282 \tag{2.6}$$

S_λ is calculated from equation 2.4, $\varepsilon_{\lambda a}$ and $\varepsilon_{\lambda c}$ are the molar extinction coefficients of PNA and the contaminant respectively, L_λ is the photon flux, and λ_{Range} is the wavelength range that was averaged. Photon flux values ranging from 297.5 to 400 nm were obtained by converting

previously reported solar irradiance values at 70°N from units of millieinsteins per centimeter squared per day (mE/cm^2/day) into millieinsteins per meter squared per nanometer (mE/m^2/nm) [82].

For experiments conducted under artificial light, apparent quantum yields were calculated using equation 2.7.

$$\varphi_{dc} = \frac{k_{dc}}{k_{da}} \frac{\sum_{240\ nm}^{400\ nm} \varepsilon_{\lambda a}}{\sum_{240\ nm}^{400\ nm} S_\lambda \varepsilon_{\lambda c}} \varphi_{da} \tag{2.7}$$

2.7. STATISTICAL ANALYSIS

Microsoft Excel 365 ProPlus was used for all statistical analyses. Associations between pairs of variables were tested with the Pearson correlation (r coefficient). Statistically significant differences between rate constants (k_{cor}) and between pairs of variables were determined at a 95% confidence interval via a student's two-tail t-test. Standard errors are reported with all associated values.

CHAPTER 3. RESULTS

3.1. DOM CHEMICAL CHARACTERISTICS

The nitrogen content of PLFA extract was about four-fold greater than the other four DOM extracts. The greatest difference in carbon content was determined to be between the Toolik Early DOM and SRFA extracts with Toolik Early DOM having 10.8% less carbon. Consistent with previous studies, the lowest carbon to nitrogen (C/N) ratio was observed for PLFA isolate (11.5) and the highest C/N ratio was observed for SRFA isolate (46.5) [66].

The FI's ranged from greatest to lowest in the following order: PLFA>Toolik Early DOM> Fog 1 DOM>Toolik Late DOM>SRFA. The relative functional group composition varied across all DOM extracts. The DOM extracts with the greatest and lowest percent composition of molecules derived from linear terpenoids (MDLT) were the Pony Lake fulvic acid extract and the Suwannee river fulvic acid extract respectively. The greatest and lowest percent composition of carboxyl rich alicyclic molecules (CRAM) was observed in the Pony Lake fulvic acid extract and Toolik Lake Late DOM respectively. The carbohydrate and peptide percent composition were greatest in the Fog 1 Lake DOM and lowest in the Pony Lake fulvic acid extract. The greatest difference in aromatic percent composition was observed between the Suwannee River fulvic acid extract and Toolik Lake Late DOM extract. Overall, the DOM extracts that had the most similar percent composition across all four of the distinct functional group categories were the Fog 1 DOM and the Toolik Lake late DOM extracts. Relative to the Toolik Late DOM extract the Toolik Early DOM extract had 3.8%, 3.2%, and 2.9% greater percent composition of MDLT, CRAM, and aromatics respectively. Alternatively, the Toolik Early DOM extract had 2.5% less carbohydrate and peptide content. Consistent with previous literature, the average percent composition of each

identified functional group region, across all DOM extracts, increased in the following order aromatics (6.5% ± 1.1) < carbohydrates and peptides (20% ± 2.9) < MDLT (26% ± 3.1) < CRAM (38.6% ± 3.7) [77] (Mitchell, et al., 2013). However, SRFA was the only extract that did not completely follow the previously described trend. The SRFA extract was determined to have a greater percent composition (1.3%) of carbohydrates and peptides relative to MDLT (Table 3.1).

Table 3.1 Chemical characteristics of DOM extracts

				^{1}H NMR Integrals as a percentage of total spectral integration from 0.3-10 ppm			
				0.6 - 1.6	*1.6 - 3.2*	*3.2 - 4.5*	*6.5 - 8.4*
Source of DOM Extract	% Carbon	% Nitrogen	FI	% MDLT	% CRAM	% Carbohydrates and Peptides	% Aromatics
Pony Lake	50.4	4.4	1.50	28.8	43.5	14.7	6.5
Suwanee River	51.1	1.1	1.33	20.8	42.3	22.1	7.8
Fog 1 Lake	49.1	1.2	1.39	28.2	36.4	22.6	6.11
Toolik Lake Early	40.3	1.0	1.43	27.9	36.9	19.1	7.5
Toolik Lake Late	46.0	1.0	1.38	24.1	33.7	21.6	4.6

3.2. PHOTODEGRADATION KINETICS OF CHLOROTHALONIL

3.2.1. DOM experiments

Consistent with previous studies chlorothalonil photodegradation was significantly enhanced, by two orders of magnitude, in the presence of fulvic acid isolates relative to experiments in 18.2 MΩ-cm water (Table 3.2).

Table 3.2 Chlorothalonil photodegradation rate constants (k_{cor}), half-lives, and quantum yields, with and without the addition of fulvic acids, under artificial solar irradiation. *a.* k_{cor} in $cm^2 \cdot J^{-1}$ *b.* half-lives in J/cm^2 *c.* Coefficient of determination calculated for the least squares fit of the degradation data to a pseudo-first order kinetics model.

Photolysis experimental conditions	k_{cor} [a]	$t_{1/2}$ [b]	Standard error of rate constant	R^2 [c]	Quantum yield
18 MΩ-cm Water	0.0004	1648.82	8.34E-05	0.5248	1.30E-05
Fog 1 DOM	0.0366	18.92	2.21E-03	0.9321	1.45E-03
Toolik Early DOM	0.0530	13.07	3.87E-03	0.8951	2.13E-03
PLFA DOM	0.0519	13.34	3.45E-03	0.9115	2.03E-03
SRFA DOM	0.0552	12.56	4.41E-03	0.8717	2.41E-03
Toolik Late DOM	0.0380	18.25	3.48E-03	0.8378	1.53E-03

All dark controls were within an average of ± 3% of the initial concentration of chlorothalonil. The average rate constant in the presence of DOM extracts was determined to be 0.0469 $cm^2 \cdot J^{-1}$ (RSD = 16.95%). The fastest degradation rate was observed in the presence of SRFA the slowest degradation rate was observed in the presence of Fog 1 DOM. There was no statistically significant difference between SRFA, PLFA, Toolik Early degradation rate constants. No statistically significant difference was observed between Fog 1 DOM and Toolik Late DOM experiments. The

average rate constant with the addition of iron was determined to be 0.0524 $cm^2 \cdot J^{-1}$ (RSD = 8.81%). Experiments conducted with the addition of iron, in the presence of fulvic acids, resulted in enhanced degradation rates for both Fog 1 DOM and Toolik Late DOM. No significant enhancement was observed in the presence of SRFA and PLFA with the addition of iron (Fig. 3.1). The quantum yields for experiments conducted in the presence of iron and Toolik Late DOM, Fog 1 DOM, PLFA, and SRFA were 1.81E-3, 2.05E-3, 2.19E-3, and 2.47E-3 respectively.

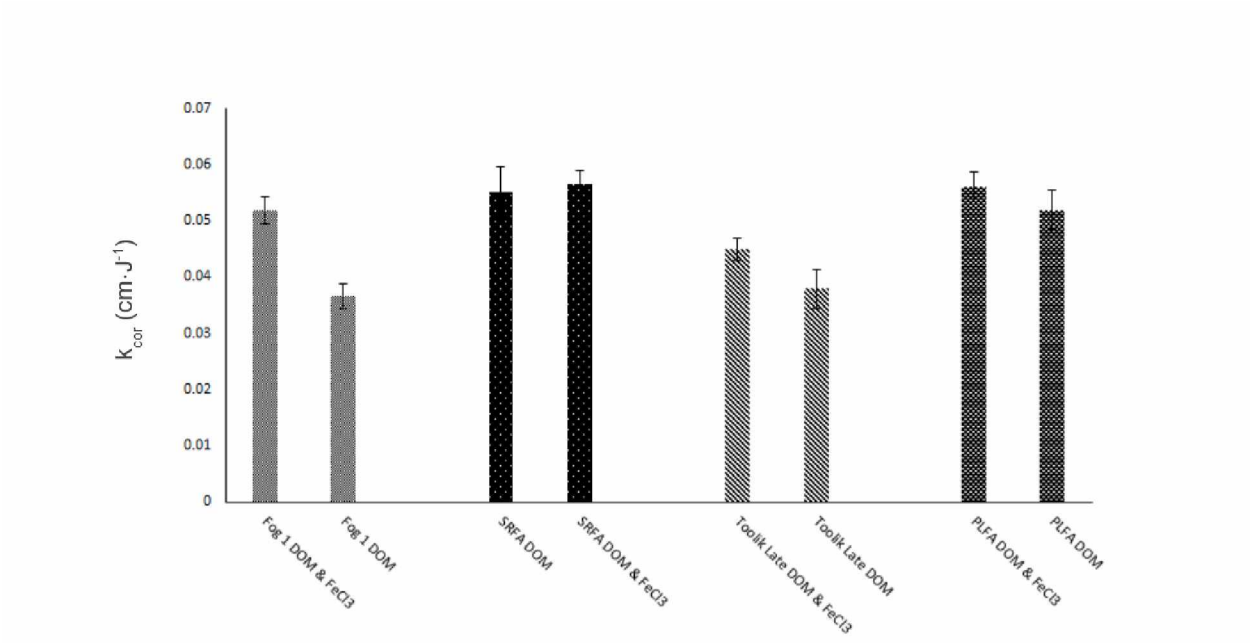

Figure 3.1 Photodegradation rate constants (k_{cor}) of chlorothalonil in the presence of different fulvic acid solutions with and without the addition of $FeCl_3$ under artificial solar irradiation. Rate constants (k_{cor}), reported with their standard error in units of $cm^2 \cdot J^{-1}$, for experiments conducted in the presence of iron are as follows: Fog 1 DOM & $FeCl_3$ (0.0519 ± 0.0024), SRFA DOM & $FeCl_3$ (0.0565 ± 0.0024), Toolik Late DOM & $FeCl_3$ (0.0450 ± 0.0019), and PLFA & $FeCl_3$ (0.0560 ± 0.0026). Rate constants for experiments conducted without the presence of iron are provided in Table 3.2.

3.3. PHOTODEGRADATION KINETICS OF CHLORPYRIFOS

3.3.1. DOM experiments

Consistent with previous studies chlorpyrifos photodegradation was enhanced in the presence of fulvic acid isolates by an average factor of two relative to experiments conducted solely in 18 MΩ-cm water (Table 3.3).

Table 3.3. Chlorpyrifos photodegradation rate constants (k_{cor}), half-lives, and quantum yields, with and without the addition of fulvic acids, under artificial solar irradiation. *a.* k_{cor} in $cm^2 \cdot J^{-1}$ *b.* half-lives in J/cm^2 *c.* Coefficient of determination calculated for the least squares fit of the degradation data to a pseudo-first order kinetics model.

Photolysis experimental conditions	k_{cor} [a]	$t_{½}$ [b]	Standard error of rate constant	R^2 [c]	Quantum yield
18 MΩ-cm Water pH 5	0.001778	389.76	9.67E-05	0.9362	1.29E-04
18 MΩ-cm Water pH 7	0.001193	580.89	5.06E-05	0.9603	8.68E-05
18 MΩ-cm Water pH 9	0.001562	443.66	5.61E-05	0.9712	1.14E-04
Fog 1 DOM pH 5	0.002676	259.00	9.64E-05	0.9747	2.16E-04
Fog 1 DOM pH 7	0.002044	338.98	9.36E-05	0.954	1.66E-04
Fog 1 DOM pH 9	0.002534	273.53	0.000103	0.9651	2.05E-04
Toolik Early DOM pH 5	0.002667	259.84	0.000169	0.9329	2.20E-04
Toolik Early DOM pH 7	0.00276	251.07	8.32E-05	0.9848	2.28E-04
Toolik Early DOM pH 9	0.00235	294.94	8.92E-05	0.9679	1.94E-04
PLFA DOM pH 5	0.001825	379.78	0.000112	0.9202	1.48E-04
PLFA DOM pH 7	0.002409	287.62	6.41E-05	0.984	1.96E-04
PLFA DOM pH 9	0.002275	304.57	9.83E-05	0.9589	1.86E-04
SRFA DOM pH 5	0.002035	340.61	6.51E-05	0.977	1.78E-04
SRFA DOM pH 7	0.002125	326.18	8.3E-05	0.9661	1.86E-04
SRFA DOM pH 9	0.002234	310.14	7.77E-05	0.9729	1.95E-04
Toolik Late DOM pH 5	0.002105	329.18	0.000105	0.9462	1.74E-04
Toolik Late DOM pH 7	0.00204	339.77	9.81E-05	0.9495	1.68E-04
Toolik Late DOM pH 9	0.001998	346.88	7.58E-05	0.9679	1.65E-04

At circumneutral pH, in the presence of fulvic acid extracts, the average rate constant was 0.0023 $cm^2 \cdot J^{-1}$ (RSD = 12.2%). The fastest rates of degradation at circumneutral pH conditions under artificial light were observed in the presence of Toolik Early and PLFA DOM isolates. The two fastest rates of degradation in the presence of PLFA and Toolik Early fulvic acids were significantly different from one another. The degradation rate constants (k_{cor}) in the presence of SRFA, Fog 1, and Toolik Late DOM were not statistically different under artificial light at circumneutral pH conditions.

Given that chlorpyrifos is susceptible to acid and base catalyzed hydrolysis within the time span of the experiments, photolysis under artificial irradiation was conducted at pH 5 and 9 to determine the influence of acidic or basic conditions on rate constants. Both acidic and basic conditions resulted in enhanced degradation relative to degradation at pH 7 for experiments conducted solely in 18.2 MΩ-cm water and in the presence of FOG 1 DOM. Under acidic and basic conditions, degradation rates in the presence of Toolik Early, Toolik Late, SRFA, and PLFA were not significantly enhanced. The average rate constant of photodegradation experiments in the presence of fulvic acids with the addition of iron was approximately twice that (k_{cor} = 0.0041 $cm^2 \cdot J^{-1}$, RSD=43.7%) of experiments without iron addition. Iron addition to DOM experiments resulted in significantly enhanced photodegradation, relative to experiments without iron addition, in the order of Fog 1 > PLFA > SRFA > Toolik Late DOM (Fig. 3.2). The quantum yields for experiments conducted in the presence of iron and Toolik Late DOM, SRFA, PLFA, and Fog 1 DOM were 2.26E-4, 2.64E-4, 2.81E-4, and 5.79E-4 respectively. All dark controls were within an average of ±10% of the initial concentration which may be a result of chlorpyrifos partitioning to the DOM. Irradiated chlorpyrifos solutions, with and without the presence of fulvic acids, were

analyzed prior to and post irradiation and left to sit in the dark for 2-7 days and re-analyzed. After being kept in the dark, all concentrations of chlorpyrifos declined by an average of 68% (RSD = 21.7%) indicating that degradation products do not revert to their parent compound.

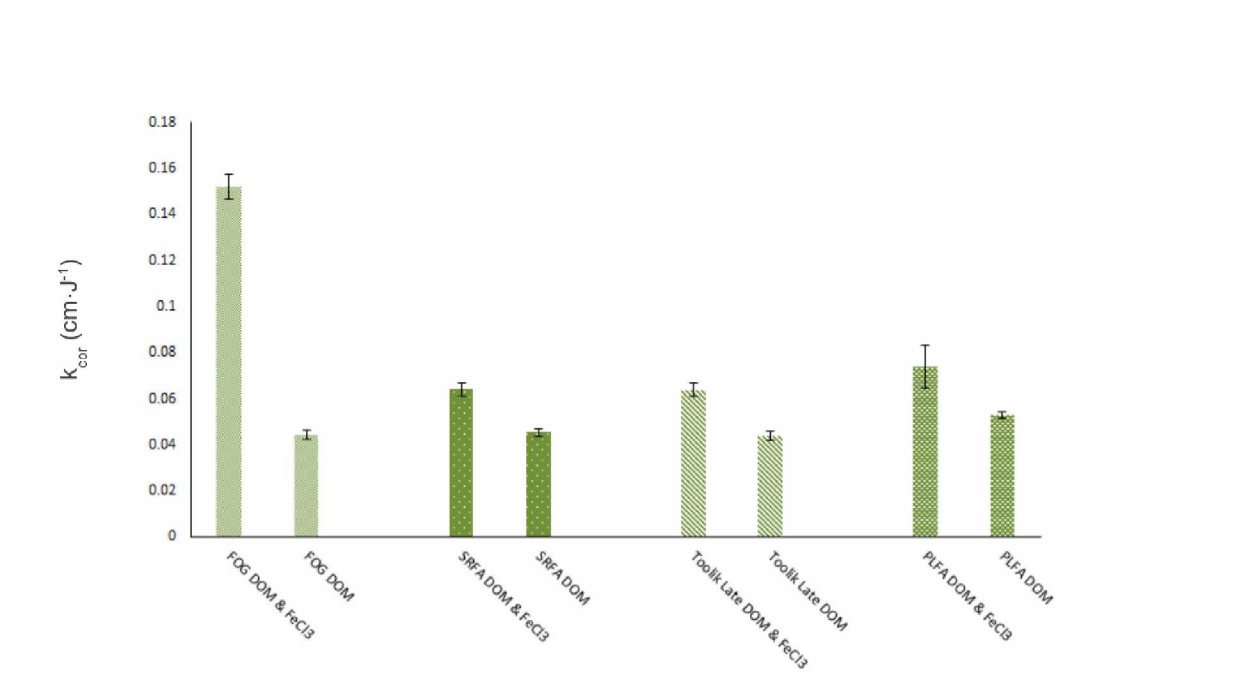

Figure 3.2 Photodegradation rate constants (k_{cor}) of chlorpyrifos in the presence of different fulvic acid solutions with and without the addition of $FeCl_3$ under artificial solar irradiation. Rate constants (k_{cor}), reported with their standard error in units of $cm \cdot J^{-1}$, for experiments conducted in the presence of iron are as follows: Fog 1 DOM & $FeCl_3$ (0.0072 ± 0.0002), SRFA DOM & $FeCl_3$ (0.0030 ± 0.0001), Toolik Late DOM & $FeCl_3$ (0.0027 ± 0.0001), and PLFA & $FeCl_3$ (0.0035 ± 0.0004). Rate constants for experiments conducted without the presence of iron are provided in Table 3.3.

3.3.2. Whole water experiments

Under natural solar irradiation, photodegradation rate constants were greater approximately by a factor of seven up to an order of magnitude in the presence of all whole waters relative to 18.2 MΩ-cm water. The average rate constant observed for whole water experiments was determined to be 0.0001 $cm^2 \cdot J^{-1}$ (RSD = 45.6%), two orders of magnitude slower than the average rate constant

in the presence of DOM isolates. The fastest rate of degradation was observed in Fog 1 Lake whole water and the slowest was observed in Toolik Lake whole water (Fig. 3.3).

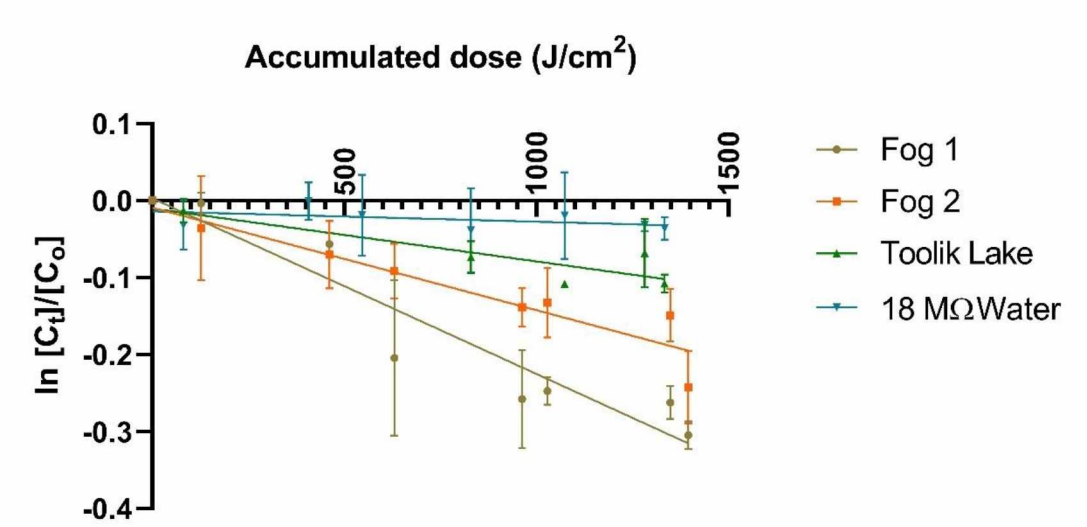

Figure 3.3 Degradation of chlorpyrifos in Arctic whole waters and in 18 MΩ-cm (18 MΩ) water under natural solar irradiation at 69°N.

All whole water photodegradation rate constants were statistically different from each other. Dark controls were an average of ± 12.4% from the initial concentration of chlorpyrifos. Although all whole waters appeared to enhance the degradation rates of chlorpyrifos, the quantum yield is lower for Toolik lake than that of the 18 MΩ-cm water. The previous finding is a reasonable given that the quantum yield calculation accounts for the wavelength specific photon flux and the extent to which a compound absorbs light at a specific wavelength. The first order rate constants (k_{cor}), half-lives, and quantum yields under artificial solar irradiation experiments are presented in Table 3.4.

Table 3.4. Photodegradation rate constants (k_{cor}), half-lives, and quantum yields in whole waters under natural solar irradiation at 69°N. *a.* k_{cor} in $cm^2 \cdot J^{-1}$ *b.* half-lives in J/cm^2 *c.* Coefficient of determination calculated for the least squares fit of the degradation data to a pseudo-first order kinetics model.

Photolysis water sources	$k_{(cor)}$ [a]	$t_{½}$ [b]	Standard error of rate constant	R^2 [c]	Quantum yield
Fog 1	2.35E-04	2949.68	2.68E-05	0.7933	1.56E-06
Fog 2	1.36E-04	5108.37	2.12E-05	0.6721	8.93E-07
Toolik Lake	7.15E-05	9696.75	1.44E-05	0.6384	6.42E-07
18 MΩ-cm Water	1.34E-05	51562.50	1.64E-05	0.0327	7.40E-07

CHAPTER 4. DISCUSSION

4.1. DOM CHEMICAL CHARACTERISTICS

Fluorescence indexes have been used to ascribe DOM as terrestrially derived (lower FI) or microbially derived (higher FI). End member fulvic acids sourced from Antarctic ponds and lakes have been reported to yield FI values ranging from 1.7-2 meanwhile, those sourced from creeks and rivers in Colorado and Georgia in the United States, yielded FI values ranging from 1.3-1.4. The FI's of the studied Arctic lakes fall within the value range established for terrestrial and microbial DOM which would suggest that the DOM in these lakes is sourced from a mix of both terrestrial and microbial sources. Furthermore, the observed FI of the Toolik Late DOM isolate is within ± 5% of the value reported by Fimmen et al. [69]. In previous literature, DOM that has been referred to as terrestrial in origin, has been characterized as being more aromatic than microbially derived DOM [66, 69, 83-84]. However, the aromaticity observed in Fog 1 DOM and in Toolik late DOM is 0.4-1.9% less than the microbial end member standard of PLFA. To our knowledge this is the first time that this has been reported and the discrepancy with prior studies, regarding the aromaticity of Toolik lake, may be due to both the natural fluctuations in the chemical composition of the DOM and experimental differences. The SRFA and PLFA end-member references, along with the Toolik Lake fulvic acids that were studied by Cory et al., were isolates extracted using NaOH as an eluent with a XAD-8 (polymethyl methacrylate) resin which does not capture the same carbon pool as PPL isolates [85]. Altogether, a direct comparison between the chemical characteristics of these distinct extracts cannot be made and the data obtained from this study is intended to be used to describe the chemical characteristics of the DOM extracts in relation to their effect on the photodegradation of chlorpyrifos and chlorothalonil. The source of microbial inputs cannot be adequately distinguished as being terrestrial or aquatic in origin and the established

generalizations regarding the chemical nature of these terms could obfuscate the findings of this study [86]. Accordingly, the terms microbial and terrestrial will not be used to further describe the Arctic DOM isolates.

The observed change of DOM functional group composition in Toolik Lake throughout the summer agrees with previous studies with respect to the temporal variation of the chemical composition of DOM [70, 87]. The greater percent composition of MDLT, CRAM, and aromatics in the earlier part of the summer could be attributed to the initial release of lignin, cyclic terpenoids, and hydroxybenzene type compounds derived from plants that were trapped during the winter in upstream tributaries and in the snow [88-89]. As the season progresses and the temperatures rise, increased microbial activity and processes like photooxidation could explain the observed decrease of MDLT, CRAM, and aromatics [88]. On the other hand, as microbial abundance and primary productivity increase throughout the summer the additional input of cellulose, plant derived glycoproteins, and bacterial polysaccharides such as peptidoglycans, would result in an increased presence of carbohydrates and peptides [86, 90-91]. To adequately discern the intra-seasonal trends of the chemical composition of Toolik Lake DOM it would be valuable to attain fulvic acid isolates over the course of multiple summers as this data set was only collected during the year of 2019.

4.2. CHLOROTHALONIL PHOTODEGRADATION

Chlorothalonil degradation experiments in the presence of DOM with the addition of $FeCl_3$ yielded a significant negative relationship between the experimentally determined rate constants (k_{cor}) and the ratio of the relative percent composition of carbohydrate and peptides to aromatic content, $r(2) = 0.95$, $p < 0.05$. For chlorothalonil degradation experiments in the presence of DOM without the addition of $FeCl_3$ a strong negative relationship was also observed between the aforementioned pair of variables but was not of statistical significance $r(3) = 0.85$, $p = 0.064$. The enhancement of

the photodegradation of chlorothalonil, in the presence of DOM with increased aromatic content relative to carbohydrates and peptides, is consistent with previous studies. Phenolic-antioxidant type molecules have been determined to have the greatest effect on the acceleration of chlorothalonil photodegradation via energy transfer reactions or by acting as electron donors that reduce chlorothalonil (CTH) (reactions 4-5) [60].

$$^3DOM^* + CTH \rightarrow {}^3CTH^* + DOM \quad (4)$$
$$^3DOM^* + CTH \rightarrow CTH^-_{+H} + DOM^-_{-H} \quad (5)$$

Greater relative abundance of aromatics in DOM has been determined to correlate with greater electron donating capacity [68]. The previous could explain why the presence of iron would strengthen the relationship between chlorothalonil rate constants and the ratio of carbohydrates and peptides to aromatics. As Fenton-type reactions cause the enhancement of degradation rates, through the increased production of hydroxyl radicals, the greater electron donating capacity in DOM could dampen the accelerating effect of iron [71, 78]. Consequently, differences between the accelerating effect of the various DOM extracts could be enhanced based on their respective aromaticity.

4.3. CHLORPYRIFOS PHOTODEGRADATION

No significant relationships between the rate constants (k_{cor}) for chlorpyrifos degradation, in the presence of DOM with and without the addition of $FeCl_3$, and the chemical characteristics of the DOM were observed. With the addition of iron, the greatest acceleration of chlorpyrifos degradation was determined in the presence of Fog 1 DOM which may be indicative that Fog 1 DOM has the lowest electron donating capacity. Hydroxyl radicals have been determined to be the second most reactive specie that contributes to the photodegradation of chlorpyrifos which may

explain why chlorpyrifos is more susceptible to degradation enhancement, with the addition of iron, relative to chlorothalonil [48].

While no statistically significant difference was determined between the degradation rate constants in the presence of Toolik Late DOM and Fog 1 DOM extracts, a statistically significant difference was observed in whole water experiments from these two sources. As the Toolik Lake whole water was extracted in closer proximity to the date of the Toolik Late DOM extract whole water, the dissolved organic matter present at the time of the whole water experiment should resemble the Toolik Late DOM extract more so than the Toolik Early DOM extract. The significant difference between rate constants in whole water experiments is likely a result of the increased basicity and ionic concentrations in Fog 1 whole water. At pH 9, Fog 1 DOM exhibited degradation enhancement relative to experiments at a circumneutral pH, indicating that basic conditions may be more favorable for indirect photolytic processes. Additionally, prior literature has established that chlorpyrifos degradation is enhanced with the increased presence of dissolved ions [41-42].

4.4. LIMITATIONS OF THE STUDY

The curvature of the quartz reaction tubes could introduce error in the observed photodegradation rates via the variable scattering of light relative to the more uniform scattering at a level surface of a lake [79, 82].

The functional group characterization of the DOM extracts via ^{1}H NMR is limited by the inability to discern the presence of highly substituted aromatics or unsaturated species as they lack protons to be detected. Additionally, the water suppression sequence SPR-5-WATERGATE can suppress up to 30% of the carbohydrate signal of any given DOM extract [92]. Accordingly, caution should

be taken upon interpreting the defined integration regions without considering them in context of all DOM extracts analyzed. Consequentially, it is more appropriate to compare the relative differences of the integral regions, between the various DOM extracts, rather than to interpret the defined integrals as absolute measures of relative functional group composition.

CHAPTER 5. CONCLUSIONS

5.1. ENVIRONMENTAL SIGNIFICANCE AND SUMMARY OF RESULTS

This study is the first to determine that DOM sourced from Arctic lakes enhances the photodegradation of both chlorpyrifos and chlorothalonil. No relationships between the degradation rates of chlorpyrifos and chlorothalonil and the relative functional group composition, FI, or C/N ratios of the DOM extracts were established. Further, a relationship between the rate constants of chlorothalonil degradation, in the presence of iron, and the percent composition ratio of carbohydrates and peptides to aromatics was observed. The previous finding, coupled with predictions of increased aromaticity and decreased hydrophilic moieties in DOM as temperatures increase, may suggest that chlorothalonil attenuation will increase accordingly [93]. At circumneutral pH, the greatest rate enhancement for chlorpyrifos degradation was observed in the presence of Toolik Early DOM. For chlorothalonil, photolytic attenuation was equally the greatest in the presence of SRFA, PLFA, and Toolik Early isolates.

Iron was found to increase the rate of degradation of chlorpyrifos in the presence of all fulvic acids by an average factor of two. Iron was only determined to significantly increase the degradation rate of chlorothalonil by an average factor of 1.3 in the presence of Fog 1 and Toolik Late DOM. The rate enhancement in the presence of iron is surmised to be a result of both the contaminant's susceptibility to hydroxyl radical degradation and to the relatively limited electron donating capacity of the DOM isolate present in solution. Faster degradation was observed for both contaminants in the presence of Toolik Early DOM relative to Toolik Late DOM which indicates that attenuation at the same source can vary throughout the spring and summer. Arctic lake water was also found to enhance the degradation rate of chlorpyrifos under natural solar irradiation at

69°N. The average half-life determined for the degradation of chlorpyrifos in Arctic lakes under field conditions ranged between 6 to 21 days and was determined to be far below predicted values for Arctic rivers [50]. The overall results of this study further support prior investigations which concluded that DOM mediated photolytic processes play an essential role in the fate of organic contaminants in Arctic environments [94]. Whole water experiments under natural solar irradiation in the Arctic revealed different results from those determined with fulvic acid experiments alone. It is therefore optimal to conduct whole water photodegradation experiments, that account for pH and the relevant concentrations of other dissolved chemical species, to obtain a more complete understanding of contaminant attenuation in natural environments.

5.2. FUTURE INVESTIGATIONS

Although statistically significant differences were determined between degradation rates, in the presence of different DOM isolates, half-lives were constrained within an order of magnitude, not exceeding a relative standard deviation (RSD) of 20%. This is consistent with previous work done in Arctic surface waters looking at the indirect photolysis of hexachlorobenzene and lindane [94]. A cursory review of the literature on the effect of fulvic acids from distinct sources on the half-lives of various compounds with distinctive functional moieties appears to show that, with the exception of ibuprofen at a concentration of 0.1 μM, the RSD between half-lives rarely exceeds 25% (Table 5.1).

Table 5.1. Half-lives and relative standard deviation (RSD%) of compound degradation in the presence of various fulvic acids.

Half-lives (hours) in the Presence of Different Fulvic Acids													
Analyte and Conditions	SRFA	PLFA	OWCFA	LFFA	LHA	UMRN	ESHA	YRFA	CRFA	HLFA	BSFA	RSD %	Source
Oxic													
BDE-153 (0.03 μM)	0.70	0.66										5.78	[95]
Sulfadimethoxide (0.1 μM)	10.51	6.20	7.02									23.62	[66]
Triclocarban (0.5 μM)	19.04	13.64	14.94									14.50	[66]
Ibuprofen (10 μM)	43.00	50.00	46.00									6.19	[96]
Ibuprofen (0.1 μM)	24.00	9.00	36.00									48.02	[96]
Metachlor (65 μM)	35.5	34.5	39.60									6.04	[95]
Metachlor (0.5 μM)	20.8	27.4	28.90									13.69	[95]
Triclocarban (0.5 μM)	19.00	13.6	14.90									14.53	[95]
Caffeine (0.1 μM)	24.75		40.76									24.44	[97]
Alachlor (5 μM)	5.73E-05			4.75E-05								9.363	[66]
Anthracene (0.28 μM)	4.62				4.95	3.47	4.07					13.17	[98]
Pyrene (0.24 μM)	7.70				7.7	7.70	4.95					16.98	[98]
Acenaphthene (0.44 μM)	0.59							0.59	0.56	0.5588	0.60	2.77	[99]
Fluorene (0.29 μM)	0.92							0.92	0.90	0.9240	0.92	1.04	[99]
Fluoranthene (0.23 μM)	1.93							1.87	1.73	1.6902	1.93	5.40	[99]
Pyrene (0.38 μM)	0.33							0.33	0.32	0.3208	0.34	1.99	[99]
Phenanthrene (0.51 μM)	0.70							0.68	0.68	0.69	0.67	0.98	[99]
Anoxic													
Ibuprofen (0.1 μM)	46.00	12.00	32.00									46.51	[96]
Ibuprofen (10 μM)	41.00		36.00									6.49	[96]
Caffeine (0.1 μM)	53.30		77.00									18.18	[97]

Given the likelihood of quantitative limits on the variability of rates and the extensive temporal and spatial variation of DOM composition, it may be more economical and practical to exclusively use a subset of readily available commercial fulvic acids to infer the relative effect of DOM on the rates of photodegradation of organic pollutants. Although DOM precursor material may be of mechanistic relevance, a cost-benefit analysis of the relative difference between observed rates of contaminant photo-degradation, with source specific isolates, is warranted to determine the relative

real-world value of these accurate measurements. If the limits on the variability of degradation rates (as they pertain to different sources of DOM) were established, commercially sourced fulvic acids could be used from the onset to determine if site-specific analysis is warranted. Depending on what quantitative regulatory limits are of concern, the determined RSD from a meta-analysis could highlight which contaminants of interest ought to be investigated for more accurate source-specific photolytic rates.

On the other hand, whole water experiments under natural solar irradiation are less resource intensive and account for a greater number of variables that are present in natural systems such as pH, metals, temperature fluctuations, and the relevant photon flux. Whole water experiments revealed different trends than experiments conducted with fulvic acid extracts, and this is likely due to the aggregate effect of the multiple variables that are not replicated in fulvic acid experiments. Whole water experiments require fewer resources and provide a more comprehensive understanding of the influence of natural waters on a contaminant's site-specific rate of degradation. Alternatively, DOM specific experiments may be of vital necessity to ascertain the effect of DOM composition on the resulting toxicity of degradation byproducts. Previous literature has shown that triclocarban degrades into different photoproducts with varying toxicity depending on the type of DOM used [65]. Although beyond the scope of this study, the identification of photoproducts would aid in the illustration of the mechanistic distinctions between the photoreactions of chlorpyrifos and chlorothalonil in the presence of the various DOM extracts. Finally, future replicate experiments investigating the role of the temporal variability in DOM sourced from Toolik lake on contaminant degradation, may provide greater insights into the seasonal trends of pollutant attenuation.

REFERENCES

1. Dikshith, T.; Diwan, P. *Organochlorine Pesticides. Industrial Guide to Chemical and Drug Safety* John Wiley & Sons, Inc. **2003**; pp. 89-122
2. Anderson, C.; Anderson, R. Suppression of superoxide production by chlorothalonil in striped bass (Morone saxatilus) macrophages: the role of cellular sulfhydryls and oxidative stress. *Aquatic Tox.* **1999**, *50*, 85-96.
3. Davies, P. Physiological, anatomic and behavioral changes in the respiratory system of Salmo gairdneri Rich. On acute and chronic exposure to chlorothalonil. *Comp Biochem Physiol.* **1986**, *88C*, 113-119.
4. Hoferkamp, L.; Hermanson, H.; Muir, C. Current use pesticides in Arctic media, 2000-2007. *Sci. Tot. Environ.* **2010**, *408 (15)*, 2985-2994.
5. Jarvinen, A.; Nordling, B.; Henry, M. Chronic toxicity of dursban (chlorpyrifos) to the fathead minnow (Pimpephales promelas) and the resultant acetylcholineesterase inhibition. *Ecotox. And Env. Safety.* **1983**, *7*, 423-434.
6. McMahon, T.; Halstead, N.; Johnson, S.; Raffel, T.; Romansic, J.; Crumrine, P.; Boughton, R.; Martin, L.; Rohr, J. The fungicide chlorothalonil is nonlinearly associated with corticosterone levels, immunity, and mortality in amphibians. *Environ. Health Perspect.* **2011**, *119 (8)*, 1098-1103.
7. Sandahal, J.; Baldwin, D.; Jenkins, J.; Scholz, N. Comparative thresholds for acetylcholinesterase inhibition and behavioral impairment in coho salmon exposed to chlorpyrifos. *Environ. Tox. And Chem.* **2004,** *24 (1)*, 136-145.
8. Tilton, F.; Bammler, T.; Gallagher, E. Swimming impairment and acetylcholinesterase inhibition in zebrafish exposed to copper or chlorpyrifos separately, or as mixtures. *Comparative Biochem. And Physiol.* **2010,** *153*, 9-16.
9. Walia, S.; Dureja, E.; Mukerjee, S. New photodegradation products of chlorpyrifos and their detection on glass, soil, and lead surfaces. *Arch. Environ. Contam. Tox.* **1988,** *17*, 183-188.
10. Williamson, S.; Moffat, C.; Gomersall, M.; Saranzewa, N.; Connolly, C.; Wright, G. Exposure to acetylcholinesterase inhibitors alters the physiology and motor function of honeybees. *Frontiers in Physiol.* **2013,** *5 (4)*, 1-10.
11. Atwood, D.; Paisley-Jones, C. *Pesticides Industry Sales and Usage : 2008-2012 Market Estimates. Report prepared for U.S. EPA.* Washington, DC: Biological and Economic Analysis Division, Office of Chemical safety and Pollution, Office of Pesticide Programs. EPA. **2017.**

12. Arvanites, A.; Boerth, D. Modeling of the mechanism of nucleophilic aromatic substitution of fungicide chlorothalonil by glutathione. *Molecular Modeling annual.* **2001,** *7 (7)*, 245-256.

13. Zhong, G.; Xie, Z.; Cai, M.; Möller, A.; Sturm, R.; Tang, J.; Ebinghaus, R. Distribution and air–sea exchange of current-use pesticides (CUPs) from East Asia to the high Arctic Ocean. *Environ. Sci. & Technol.* **2011,** *46 (1)*, 259-267.

14. Ruggirello, R.; Hermanson, M.; Isaksson, E.; Teixeira, C.; Forsström, S.; Muir, D.; Pohjola, V.; Wal, R.; Meijer, H. Current use and legacy pesticide deposition to ice caps on Svalbard, Norway. *J. Geophs. Res.* **2010,** *115*, D18308.

15. Chishtia, Z.; Hussain, S.; Arshada, K.; Khalid, A.; Arshada, M. Microbial degradation of chlorpyrifos in liquid media and soil. *J. of Environ. Manag.* **2013,** *114 (15)*, 372-380.

16. Scheringer, M. Long-range transport of organic chemicals in the environment. *Environ. Tox. & Chem.* **2009,** *28 (4)*, 677-690.

17. Tan, Y.; Xiong, H.; Shi, T.; Hua, R.; Wu, X.; Cao, H.; Li, X.; Tang, J. Photosensitizing Effects of Nanometer TiO2 on Chlorothalonil Photodegradation in Aqueous Solution and on the Surface of Pepper. *J. Agric. Food Chem.* **2013,** *61 (21)*, 5003-5008.

18. Balmer, J.; Morris, A.; Hung, H.; Jantunen, L.; Vorkamo, K.; Riget, F.; Evans, M.; Houde, M.; Muir, D. Levels and trends of current-use pesticides (CUPs) in the arctic: An updated review, 2010-2018. *Emerging contaminants.* **2019,** *5*, 70-88.

19. Muir, D.; Teixeira, C.; Wania, F. Empirical And Modeling Evidence Of Regional Atmospheric Transport Of Current-Use Pesticides. *Environ.Toxicol. and Chem.* **2004,** *23 (10)*, 2421.

20. Pućko, M.; Stern, G.; Burt, A.; Jantunen, L.; Bidleman, T.; Macdonald, R.; Barber, D.; Geilfus, N.; Rysgaard, S. Current use pesticide and legacy organochlorine pesticide dynamics at the ocean-sea ice-atmosphere interface in Resolute Passage, Canadian Arctic, during winter-summer transition. *Sci. Total Environ.* **2017,** *580*, 1460-1469.

21. Comiso, J.; Parkinson, C.; Gersten, R.; Stock, L. Climate accelerated decline in the Arctic sea ice cover. *Geophys. Res. Letters.* **2008,** *35 (1)*, L01703.

22. Pućko, M.; Stern, G.; Macdonald, R.; Jantunen, L.; Bidleman, T.; Wong, F.; Barber, D.; Rysgaard, S. The delivery of organic contaminants to the Arctic food web: Why sea ice matters. *Sci. Total Environ.* **2014,** *506-507*, 444-452.

23. Morris, A.; Muir, D.; Solomon, K.; Letcher, R.; McKinney, M.; Fisk, A.; Duric, M. Current-use pesticides in seawater and their bioaccumulation in polar bear-ringed seal food chains of the Canadian Arctic. *Environ. Tox. And Chem.* **2016,** *35 (7)*, 1695-1707.

24. Morris, A.; Solomon, K.; Muir, D.; Teixeira, C. Trophodynamics of current use pesticides and ecological relationships in the Bathurst Region vegetation-caribou-wolf food chain of the Canadian Arctic. *Environ. Tox. And Chem.* **2014,** *33 (9)*, 1956-1966.

25. Lallement, G.; Dorandeu, F.; P. Filliat, P.; Carpentier, P.; Baille, V.; Blanchet, G.; Medical management of organophosphate-induced seizures. *J. Physiol. Pari.* **1998,** *92*, 369-373.

26. Jarvinen, A.; Nordling, B.; Henry, M. Chronic toxicity of dursban (chlorpyrifos) to the fathead minnow (Pimpephales promelas) and the resultant acetylcholineesterase inhibition. *Ecotox. And Env. Safety.* **1983,** *7*, 423-434.

27. Sandahal, J.; Baldwin, D.; Jenkins, J.; Scholz, N. Odor-evoked field potentials as indicators of sublethal neurotoxicity in juvenile coho salmon (Oncorhynchus kisutch) exposed to copper, chlorpyrifos, or estenvalerate. *Can. J. Fish. Aquat. Sci.* **2003,** *61*, 404-413.

28. Slotkin, T.; Seidler, F.; Fumagalli, F. Exposure to organophosphates reduces the expression of neurotrophic factors in neonatal rat brain regions: similarities and differences in the effects of chlorpyrifos and diazinon on the fibroblast growth factor superfamily. *Env. Health Perspect.* **2007,** *115 (6)*, 909-916.

29. Howard, A.; Bucelli, R.; Jett, D.; Bruun, D.; Yang, D.; Lein, P. Chlorpyrifos exerts opposing effects on axonal and dendritic growth in primary neuronal cultures. *Tox. And Applied Pharma.* **2005,** *207*, 112-124.

30. Jett, D.; Navoa, R.; Beckles, R.; McLemore, G. Cognitive function and cholinergic neurochemistry in weanling rats exposed to chlorpyrifos. *Tox. And applied Pharma.* **2001,** *(174)*, 89-98.

31. Slotkin, T.; Card, J.; Seidler, F. Chlorpyrifos developmental neurotoxicity: interaction with glucocorticoids in PC12 cells. *Neurotoxicol Teratol.* **2012,** *34 (5)*, 505-512.

32. Chadwick, J.; Nislow, K.; McCormick, S. Thermal onset of cellular and endocrine stress responses correspond to ecological limits in brook trout, an iconic cold-water fish. *Conservation Physio.* **2015,** *3*, 1-12.

33. Rush, T.; Hjelmhaug, L.; Lobner, D. Mechanisms of chlorpyrifos and diazinon induced neurotoxicity in cortical culture. *Neurosci.* **2010,** *116*, 899-906.

34. Bessi, H.; Cossu-Leguille, C.; Vasseur, Z. Effects of chlorothalonil on glutathione and glutathione-dependent enzyme activities in syrian hamster embryo cells. *Environ. Contam. Tox.* **1999,** *63*, 582-589.

35. Lebailly, P.; Vigreux, C.; Godard, T.; Sichel, F.; Bar, E.; LeTalaer, J.; Henry-Amar, M.; Gauduchon, P. Assessment of DNA damage induced in vitro by etoposide and two fungicides (carbendazim and chlorothalonil) in human lymphocytes with the comet assay. *Mutation Research.* **1997,** *375*, 205-217.

36. Zhong, H.; Yazdanbakhsh, K. Hemolysis and immune regulation. *Current Opinion Hematol.* **2018,** *25 (3)*, 177-182.

37. Schmidtko, S.; Stramma, L.; Visbeck, M. Decline in global oceanic oxygen content during the past five decades. *Nature.* **2017,** *542*, 335-339.

38. Singh, B.; Walker, A.; Morgan, J.; Wright, D. Biodegradation of chlorpyrifos by Enterobacter strain B-14 and its use in bioremediation of contaminated soils. *Applied and Environ. Microbio.* **2004,** *70*, 4855-4863.

39. Anwar, S.; Liaquat, F.; Khan, Q.; Khalid, Z.; Iqbal, S. Biodegradation of chlorpyrifos and its hydrolysis product 3,5,6-trichloro-2-pyridinol by bacterial strain C2A1. *J. Hazardous Materials.* **2009,** *168*, 400-405.

40. Racke, K.; Laskowski, D.; Schultz, M. Resistance of chlorpyrifos to enhanced biodegradation in soil. *J. Agric. Food Chem.* **1990,** *38*, 1430-1436.

41. Marouane, B.; Hajjaji, S.; Yadini, A.; Dahchour, A. Photolysis of chlorpyrifos in various aqueous solutions. *J. Agric. Sci. & Review.* **2015,** *4 (8)*, 239-245.

42. Meikle, R.; Youngson, C. The hydrolysis rate of chlorpyrifos, o-o-diethyl o-(3,5,6-trichloro-2-pyridyl) phosphorothioate, and its dimethyl analog, chlorpyrifos-methyl, in dilute aqueous solution. *Arch. Environ. Contam. Toxicol.* **1978,** *7*, 13-22.

43. Noblet, J.; Smith, L.; Suffet, I. Influence of natural dissolved organic matter, temperature, and mixing on the abiotic hydrolysis of triazine and organophosphate pesticides. *J Agric Food Chem.* **1996,** *44*, 3685–3693.

44. Meikle, R.; Kurihara, N.; DeVries, D. Chlorpyrifos: The photodecomposition rates in dilute aqueous solution and on a surface, and the volatilization rate from a surface. *Arch. Environ. Contam. Toxicol.* **1983,** *12*, 189-193.

45. Muhamad, S. Kinetic studies of catalytic photodegradation of chlorpyrifos insecticide in various natural waters. *Arabian J. Chem.* **2010,** *3*, 127-133.

46. Penuela, G.; Barcelo, D. Comparative degradation kinetics of chlorpyrifos in water by photocatalysis using solid-phase disk extraction followed by gas chromatographic techniques. *Toxicol. Environ. Chem.* **1997,** *62 (1)*, 135-147.

47. Pinto, M.; Salgado, R.; Cottrell, B.; Cooper, W.; Burrows, H.; Vale, C.; Sontag, G.; Noronha, J. Influence of dissolved organic matter on the photodegradation and volatilization kinetics of chlorpyrifos in coastal waters. *J. Photochem. Photobiol. A: Chem.* **2015,** *310*, 189-196.

48. Zeng, T.; Arnold, W. Pesticide photolysis in Prarie Potholes: probing photosensitized processes. *Environ. Sci. Tecnol.* **2013,** *47 (13)*, 6735-6745.

49. Rosario-Ortiz, F.; Canonica, S. Probe compounds to assess the photochemical activity of dissolved organic matter. *Environ. Sci. Technol.* **2016,** *50*, 12532-12547.

50. Dilling, W.; Lickly, L.; Lickly, T.; Murphy, P. Quantum yields for O,O-diethylO-(3,5,6-trichloro-2-pyridinyl) phosphorothioate (chlorpyrifos) and 3,5,6-trichloro-2-pyridinol in dilute aqueous solutions and their environmental phototransformation rates. *Environ. Sci. Technol.* **1984**, *18*, 540-543.

51. George, M.; Bhat, V. Photoxigenations of nitrogen heterocycles. *Chem Reviews.* **1979,** *79 (5)*, 447-478.

52. Smith, G. Ultraviolet light decomposition studies with DURSBAN and 3,5,6-trichloro-2-pyridinol. *J. Economic Entomology.* **1968,** *61 (1)*, 793-799.

53. Eeden, M.; Potgieter, H.; Walt, A. V. Microbial degradation of chlorothalonil in agricultural soil: a laboratory investigation. *Environ. Tox.* **2000,** *15*, 533-539.

54. Xiaoquang, C.; Hua, F.; Xuedong, P.; Xiao, W.; Min, S.; Bo, F.; Yunlong, Y. Degradation of chlorpyrifos alone and in combination with chlorothalonil and their effects on soil microbial populations. *J. Environ. Sci.* **2008,** *20 (4)*, 464-469.

55. Liang, B.; Li, R.; Jiang, D.; Sun, J.; Qiu, J.; Zhao, Y.; Li, S.; Jiang, J. Hydrolytic Dechlorination of Chlorothalonil by Ochrobactrum sp. CTN-11 Isolated from a Chlorothalonil-Contaminated Soil. *Current microbiology.* **2010,** *61*, 266-233.

56. Kwon, J.; Armbrust, K. Degradation of chlorothalonil in irradiated water/sediment systems. *J.Agric. Food Chem.* **2006,** *54*, 3651-3657.

57. Shibamoto, T. Effect of pH on the hydrolysis of chlorothalonil. *J.Agric. Food Chem.* **1977,** *25 (1)*, 208-210.

58. Szalkowski, M.; Stallard, D. Effect of pH on the hydrolysis of chlorothalonil. *J. Agric. Food Chem.* **1977,** *25 1* , 208-210.

59. Penuela, G.; Barcelo, D. Photodegradation and stability of chlorothalonil in water studied by solid-phase disk extraction, followed by gas chromatographic techniques. *J. Chromatogra. A.* **1998,** *823*, 81-90.

60. Porras, J.; Fernandez, J.; Torres-Palma, R.; Richard, C. Humic substances enhance chlorothalonil phototransformation via photoreduction and energy transfer. *Environ. Sci. Technol.* **2014,** *48*, 2218-2225.

61. Sakkas, V.; Lambropoulou, D.; Albanis, T. Study of chlorothalonil photodegradation in natural waters and in the presence of humic substances. *Chemosphere.* **2002,** *48*, 939-945.

62. Bouchama, S.; Sainte-Claire, P.; Arzoumanian, E.; Oliveros, E.; Boulkamh, A.; Richard, C. Photoreactivity of the fungicide chlorothalonil in aqueous medium. *Environ. Sci.: Processes Impacts.* **2014,** *16*, 839-847.

63. Comiso, C.; Hall, D. Climate trends in the arctic as observed from space. *Wiley Interdiscip. Rev. Clim. Change.* **2014,** *5 (3)*, 389-409.

64. Guo, L.; Ping, C. Macdonald, R.W. Mobilization pathways of organic carbon from permafrost to arctic rivers in a changing climate. *Geophys. Res. Letters.* **2007,** *34 (13)*, L13603.

65. Albanese, K. A.; Lanno, R. P.; Hadad, C. M.; Chin, Y.-P. Photolysis- and Dissolved Organic Matter-Induced Toxicity of Triclocarban to Daphnia magna. *Environmental Science and Technology Letters.* **2017,** *4 (11)*, 457-462.

66. Guerard, J. J.; Miller, P. L.; Trouts, T. D.; Chin, Y.-P. The role of fulvic acid composition in the photosensitized degradation of aquatic contaminants . *Aquat. Sci.* **2009,** *71*, 160-169.

67. Wenk, J. The role of dissolved organic matter in aquatic photochemical oxidation processes. *Doctoral Thesis. ETH Zürich.* **2012.**

68. Aeschbacher, M.; Graf, C.; Schwarzenbach, R. P.; Sander, M. Antioxidant properties of humic substances . *Environ. Sci. Technol.* **2012,** *46*, 4916-4925.

69. Fimmen, R. L.; Cory, R. M.; Chin, Y.-P.; Trouts, T. D.; Mcknight, D. M. Probing the oxidation-reducation properties of terrestrially and microbially derived dissolved organic matter. *Geochimica et Cosmochimica Acta.* **2007,** *71*, 3003-3015.

70. Gagne, K. R.; Ewers, S. C.; Murphy, C. J.; Daanen, R.; Anthony, K. W.; Guerard, J. J. Composition and photo-reactivity of organic matter from permafrost soils and surface waters in interior Alaska. *Environ. Sci.: Processes and Impacts* **2020,** *22*, 1525-1539.

71. Trusiak, A.; Treibergs, L. A.; Kling, G. W.; Cory, R. M. The role of iron and reactive oxygen species in the production of co2 in arctic soil waters. *Geochimica et Cosmochimica Acta.* **2018,** *224*, 80-95.

72. Gouin, T.; Cousins, I.; Mackay, D. Comparison of two methods for obtaining degradation half-lives. *Chemosphere.* **2004,** *56*, 531-535.

73. Hinkel, K.; Nelson, F. Spatial and temporal patterns of active layer thickness at Circumpolar Active Layer Monitoring (CALM) sites in northern Alaska, 1995–2000. *J. Geophys.Res.* **2003,** *108*, 8168.

74. Williams, M.; Rastetter, E. B. Vegetation characteristics and primary productivity along an arctic transect: implications for scaling-up. *J. of Ecology.* **2001,** *87*, 885-898.

75. Arp, C. D.; Jones, B. M.; Liljedahl, A. K.; Hinkel, K. M.; Welker, J. A. Depth, ice thickness, and ice-out timing cause divergent hydrologic responses among Arctic lakes. *Water Resour. Res.* **2015,** *51*, 9379– 9401.

76. Keller, K.; Blum, J. D.; Kling, G. W. Stream geochemistry as an indicator of increasing permafrost thaw depth in an arctic watershed. *Chem. Geology.* **2010,** *273*, 76-81.

77. Mitchell, P. J.; Simpson, A. J.; Soong, R.; Oren, A.; Chefetz, B.; Simpson, M. J. Solution-state NMR investigation of the sorptive fractionation of dissolved organic matter by alkaline mineral soils. *Environ. Chem.* **2013,** *10*, 333-340.

78. Cooper, W. J.; Zika, R. G.; Petasne, R. G.; Plane, J. M. Photochemical formation of H2O2 in natural waters esposed to sunlight. *Environ. Sci. Technol.* **1988,** *22*, 1156-1160.

79. Dulin, D.; Mill, T. Development and evaluation of sunlight actinometers. *Environ. Sci. Technol.* **1982,** *16*, 815-820.

80. Wei-Haas, M.; Chin, Y. A fluence-based method for the direct comparison of photolysis kinetics under variable light regimes. *Environ. Sci. Technol.* **2015,** 2 (7), 183-187.

81. Miller, P. L.; Chin, Y. Photoinduced degradation of carbaryl in wetland surface water. *J. Agric. Food Chem.* **2002,** 6758-6765.

82. Leifer, A. *The Kinetics of Enviornmental Aquatic Photochemistry: Theory and Practice.* York, PA: American Chemical Society. **1988.**

83. Cawley, K. M.; McKnight, D. M.; Miller, P.; Cory, R.; Fimmen, R. L.; Guerard, J.; Dieser, M.; Jaros, C.; Chin, Y.; Foreman, C. Characterization of fulvic acid fractions of dissolved organic matter during ice-out in a hyper-eutrophic, coastal pond in Antarctica. *Environ. Res. Lett.* **2013,** *8*, 045015.

84. Mladenov, N.; McKnight, D. M.; Macko, S. A.; Norris, M.; Cory, R. M.; Ramerg, L. Chemical characterization of DOM in channels of a seasonal wetland. *Aquat. Sci.* **2007,** *69*, 456-471.

85. Perminova, I.; Dubinenkov, I.; Kononikhin, A.; Konstantinov, A.; Zherebker, A.; Andzhushev, M.; Mantsa A.; Lebedev, V.; Bulygina, E.; Holmes, R.; Kostyukevich, Y.; Popov, I.; Nikolaev, E. Molecular mapping of sorbent selectivities with respect to isolation of Arctic dissolved organic matter as measured by fourier transform mass spectrometry. *Environ. Sci. Technol.* **2014,** *48*, 7461-7468.

86. McCaul, M.; Sutton, D.; Simpson, A.; Spence, A.; McNally, D.; Moran, B.; Brian, W.; Goel, A.; O'Connor, B.; Hart, K. Composition of dissolved organic matterwithin a lacustrine environment. *Environ. Chem.* **2011,** *8*, 146-154.

87. Jaffe, R.; McKnight, D.; Maie, N.; Cory, R.; McDowell, W. H.; Campell, J. L. Spatial and temporal variations in DOM composition in ecosystems: The importance of long-term monitoring of optical properties. *J. of Geophy. Research.* **2008,** *113*, G04032.

88. Awad, J.; Leeuwen, J. v.; Chow, C. W.; Smernik, R. J.; Anderson, S. J.; Cox, J. W. Seasonal variation in the nature of DOM in a river and drinking water reservoir of a closed catchment. *Environ. Pollution.* **2017,** *220*, 788-796.

89. Kaiser, K.; Canedo-Oropeza, M.; McMahon, R.; Amon, R. M. Origins and transformations of dissolved organic matter in large Arctic rivers. *Sci. Rep.* **2017,** *7*, 13064.

90. Garneau, M.; Roy, S.; Lovejoy, C.; Gratton, Y.; Vincent, W. Seasonal dynamics of bacterial biomass and production in a coastalarctic ecosystem: Franklin Bay, western Canadian Arctic. *Journal of Geophysical Research.* **2008,** *113*, C07S91.

91. Hobbie, J.; Corliss, T.; Peterson, B. Seasonal patterns of bacterial abundance in an Arctic lake. *Arctic and Apline Research.* **1983,** *15:2*, 253-259.

92. Lam, B.; Simpson, A. J. Direct 1H NMR spectroscopy of dissolved organic matter in natural waters. *Analyst.* **2008,** *133*, 263-269.

93. O'Donnell, J. A.; Aiken, G. R.; Butler, K. D.; Guillemette, F.; Podgorski, D. C.; Spencer, R. G. DOM composition and transformation in boreal forest soils: The effects of temperature and organic-horizon decomposition state. *J. Geophs. Res. Biogeosci.* **2016,** *121*, 2727-2744.

94. Grannas, A. M.; Cory, R. M.; Miller, P. L.; Chin, Y.-P.; McKnight, D. M. The role of dissolved organic matter in arctic surface waters in the photolysis of hexachlorobenzene and lindane. *J. Geophys. Res.* **2012,** *117*, G01003.

95. Wang, H.; Wang, M.; Wang, H.; Gao, J.; Dahlgren, R. A.; Yu, Q.; Wang, X. Aqueous photochemical degradation of BDE-153 in solutions withnatural dissolved organic matter. *Chemosphere.* **2016,** *155*, 367-374.

96. Jacobs, L.; Fimmen, R.; Chin, Y.; Mash, M.; Weavers, L. Fulvic acid mediated photolysis of ibuprofen in water. *Water Res.* **2011,** *45 (15)*, 4449-4458.

97. Jacobs, L.; Weavers, L.; Houtz, E.; Chin, Y. Photosensitized degradation of caffeine: Role of fulvic acids and nitrate. *Chemosphere.* **2012,** *86 (2)* , 124-129.

98. Zhao, S.; Xue, S.; Zhang, J.; Zhang, Z.; Sun, J. Dissolved organic matter-mediated photodegradation of anthracene and pyrene in water. *Scientific Rep.* **2020,** *10*, 3413.

99. Xia, X.; Li, G.; Yang, Z.; Chen, Y.; Huang, G. Effects of fulvic acid concentration and origin on photodegradation of polycyclic aromatic hydrocarbons in aqueous solution: importance of active oxygen. *Environ. Pollut.* **2009,** *157 (4)*, 1352-1359.

APPENDIX A. METHODS

Table A.2.1. Percent recovery of dissolved carbon from whole waters after DOM extraction. *a.* Calculated as the product of the dissolved carbon concentration in mg/L in whole waters by the total liters of water extracted *b.* Recovery greater than 100% is possibly due to the inaccurate determination of volume extracted.

DOM Extract Source	Total expected carbon in extracts (mg)[a]	Grams of DOM extracted	Milligrams Carbon per gram of DOM extract	Percent recovery (%)
FOG 1	395.4	0.842	491.470	104.7[b]
Toolik (5/19)	168.3	0.301	402.846	72.1
Toolik (7/19)	1227.4	1.201	459.900	45.0

Table A.2.2. Time points and respective accumulated dose values at which irradiated solutions of chlorpyrifos, in whole waters at 69°N, were removed and stored in the dark until analysis.

Fog 1 and Fog 2		*Toolik Lake*		*18 MΩ-cm Water*	
Time (hours)	Accumulated Dose (J/cm^2)	Time (hours)	Accumulated Dose (J/cm^2)	Time (hours)	Accumulated Dose (J/cm^2)
0.00	0.00	0.00	0.00	0.00	0.00
4.50	127.19	3.67	80.91	3.67	80.91
20.23	461.42	44.13	829.93	16.47	406.76
27.83	630.35	54.97	1073.70	28.05	546.23
43.43	963.27	65.80	1282.02	44.13	829.93
46.67	1028.43	69.87	1334.02	54.97	1073.70
59.07	1348.55			65.80	1282.02
62.32	1395.35			69.87	1334.02

Table A.2.3. Time points and respective accumulated dose values at which irradiated solutions of chlorpyrifos, under artificial solar irradiation, were removed and stored in the dark until analysis.

Toolik Late DOM pH 5		*Toolik Late DOM pH 7*		*Toolik Late DOM pH 9*		*Toolik Late DOM & $FeCl_3$*	
Time (hours)	Accumulated Dose (J/cm^2)	Time (hours)	Accumulated Dose (J/cm^2)	Time (hours)	Accumulated Dose (J/cm^2)	Time (hours)	Accumulated Dose (J/cm^2)
0.00	0.00	0.00	0.00	0.00	0.00	0.00	0.00
1.00	20.90	1.00	20.66	1.00	20.48	1.00	21.10
2.00	42.02	2.00	41.65	2.00	41.37	2.00	41.94
3.00	63.15	3.00	62.64	3.00	62.27	3.00	62.68
6.00	126.95	6.00	126.86	6.00	125.51	4.00	83.77
18.00	383.84	18.18	386.54	18.08	392.61	5.00	104.87

Table A.2.3. continued

24.00	512.28	24.18	514.42	24.08	525.24	7.00	147.06
32.00	685.40	32.02	683.20	32.00	695.08	10.00	211.43
48.30	1040.40	47.70	1030.61	48.08	1045.29	24.00	559.69

Fog 1 DOM pH 5		*Fog 1 DOM pH 7*		*Fog 1 DOM pH 9*		*FOG DOM & $FeCl_3$*	
Time (hours)	Accumulated Dose (J/cm^2)	Time (hours)	Accumulated Dose (J/cm^2)	Time (hours)	Accumulated Dose (J/cm^2)	Time (hours)	Accumulated Dose (J/cm^2)
0.00	0.00	0.00	0.00	0.00	0.00	0.00	0.00
1.00	20.43	1.00	20.38	1.00	20.62	1.00	20.20
2.00	41.28	2.00	41.19	2.07	43.29	2.00	40.54
3.00	62.13	3.00	61.99	3.07	64.56	3.00	61.02
6.00	125.65	6.00	127.05	6.00	125.73	4.00	81.58
18.17	394.02	18.00	384.49	18.10	390.94	5.00	102.13
24.18	526.74	24.02	513.57	24.10	522.45	7.00	143.24
32.01	696.43	32.02	694.13	32.00	698.92	10.00	207.29
		48.02	1045.57	48.00	1042.17	24.00	507.67

PLFA DOM pH 5		*PLFA DOM pH 7*		*PLFA DOM pH 9*		*PLFA DOM & $FeCl_3$*	
Time (hours)	Accumulated Dose (J/cm^2)	Time (hours)	Accumulated Dose (J/cm^2)	Time (hours)	Accumulated Dose (J/cm^2)	Time (hours)	Accumulated Dose (J/cm^2)
0.00	0.00	0.00	0.00	0.00	0.00	0.00	0.00
1.00	21.22	1.03	21.59	1.00	21.04	1.00	19.94
2.08	44.31	1.97	41.66	2.00	42.67	2.00	39.96
3.08	65.62	3.00	63.88	3.00	64.31	3.00	60.37
6.05	129.41	6.82	144.69	6.00	130.07	4.00	80.96
18.56	404.19	18.03	385.33	18.32	401.74	5.00	101.56
24.60	536.86	23.97	512.62	24.32	534.09	7.00	142.74
32.08	701.58	32.02	690.94	32.00	704.65	10.00	205.27
46.32	1020.84	48.03	1058.39	47.90	1062.03	24.00	504.14

SRFA DOM pH 5		*SRFA DOM pH 7*		*SRFA DOM pH 9*		*SRFA DOM & $FeCl_3$*	
Time (hours)	Accumulated Dose (J/cm^2)	Time (hours)	Accumulated Dose (J/cm^2)	Time (hours)	Accumulated Dose (J/cm^2)	Time (hours)	Accumulated Dose (J/cm^2)
0.00	0.00	0.00	0.00	0.00	0.00	0.00	0.00
1.00	21.04	1.00	20.43	1.00	20.52	1.00	19.48
2.00	42.16	2.00	40.77	2.00	41.70	2.00	39.46
3.00	63.29	3.00	61.11	3.00	62.87	3.00	59.69
6.00	129.33	6.00	123.79	6.00	125.84	4.00	80.24
18.00	386.21	18.12	379.79	18.58	403.99	5.00	100.80
24.00	514.65	24.12	506.56	24.58	536.62	7.00	141.91

Table A.2.3. continued

32.00	687.40	32.22	680.34	32.00	698.14	10.00	206.28
48.00	1038.84	47.98	1024.45	48.00	1047.35	24.00	507.67

Toolik Early DOM pH 5		*Toolik Early DOM pH 7*		*Toolik Early DOM pH 9*	
Time (hours)	Accumulated Dose (J/cm^2)	Time (hours)	Accumulated Dose (J/cm^2)	Time (hours)	Accumulated Dose (J/cm^2)
0.00	0.00	0.00	0.00	0.00	0.00
1.00	21.17	1.00	21.13	1.00	21.50
2.00	41.74	2.00	42.63	2.00	43.33
3.00	62.31	3.00	64.13	3.00	65.15
6.00	124.86	6.00	128.35	6.00	130.21
18.00	376.72	18.23	395.92	18.00	399.93
24.00	502.66	24.23	527.15	24.00	534.79
32.02	676.88			32.00	715.72
48.00	1036.13			48.00	1082.04

18 MΩ-cm Water pH 5		*18 MΩ-cm Water pH 7*		*18 MΩ-cm Water pH 9*	
Time (hours)	Accumulated Dose (J/cm^2)	Time (hours)	Accumulated Dose (J/cm^2)	Time (hours)	Accumulated Dose (J/cm^2)
0.00	0.00	0.00	0.00	0.00	0.00
1.00	21.45	1.00	21.97	1.00	21.59
2.00	43.37	2.00	44.44	2.00	42.77
3.00	65.29	3.00	66.92	3.00	63.94
6.40	140.13	6.00	132.67	6.00	128.72
17.82	392.49	18.00	395.70	18.18	397.46
24.25	534.70	24.00	527.21	24.18	529.81
32.03	704.57	32.00	709.63	32.00	704.78
50.42	1110.08	48.00	1067.02	48.20	1070.41

Table A.2.4. Time points and respective accumulated dose values at which irradiated solutions of chlorothalonil, at pH 7 under artificial solar irradiation, were removed and stored in the dark until analysis.

18 MΩ-cm Water		*Early Toolik DOM*		*Late Toolik DOM*	
Time (hours)	Accumulated Dose (J/cm^2)	Time (hours)	Accumulated Dose (J/cm^2)	Time (hours)	Accumulated Dose (J/cm^2)
0.00	0.00	0.00	0.00	0.00	0.00
0.25	5.11	0.25	5.06	0.25	5.14

Table A.2.4. continued

0.50	10.31	0.50	10.22	0.51	10.43
1.00	20.71	1.01	21.00	0.99	20.94
1.50	31.18	1.50	30.93	1.50	31.42
2.00	41.58	2.00	41.24	2.01	41.85
2.50	52.03	2.50	51.57	2.50	51.79
3.00	62.43	3.01	62.36	3.00	62.61
4.00	83.42	4.00	83.77	4.00	83.78

FOG DOM		*PLFA DOM*		*SRFA DOM*	
Time (hours)	Accumulated Dose (J/cm^2)	Time (hours)	Accumulated Dose (J/cm^2)	Time (hours)	Accumulated Dose (J/cm^2)
0.00	0.00	0.00	0.00	0.00	0.00
0.50	10.08	0.26	5.31	0.26	5.02
1.03	20.70	0.50	10.40	0.50	9.90
1.53	30.80	1.00	20.89	1.00	20.03
2.00	40.46	1.50	31.09	1.50	30.12
2.50	50.79	2.00	41.53	2.00	40.12
3.50	71.69	2.50	52.03	2.50	50.14
4.00	82.14	3.00	62.52	3.00	60.27
5.50	113.46	4.00	83.79	4.00	81.08

FOG DOM & $FeCl_3$		*Toolik Late DOM & $FeCl_3$*		*PLFA DOM & $FeCl_3$*		*SRFA DOM & $FeCl_3$*	
Time (hours)	Accumulated Dose (J/cm^2)	Time (hours)	Accumulated Dose (J/cm^2)	Time (hours)	Accumulated Dose (J/cm^2)	Time (hours)	Accumulated Dose (J/cm^2)
0.00	0.00	0.00	0.00	0.00	0.00	0.00	0.00
0.08	1.64	0.09	1.84	0.08	1.65	0.07	1.46
0.17	3.28	0.17	3.37	0.17	3.33	0.18	3.62
0.25	4.92	0.26	5.21	0.25	4.98	0.25	5.07
0.50	10.06	0.50	10.16	0.50	10.23	0.50	10.34
0.75	15.18	0.75	15.42	0.75	15.38	0.75	15.54
1.00	20.36	1.00	20.66	1.00	20.93	1.00	20.72
1.50	30.65	1.50	30.94	1.50	31.42	1.50	31.26
2.00	41.08	2.00	41.41	2.00	42.30	2.00	41.73

APPENDIX B. RESULTS

Table B.3.1. Chlorothalonil photodegradation pseudo first-order rate constants (k_{cor}) and half-lives in units of time, with and without the addition of fulvic acids, under artificial and natural solar irradiation. *a.* k_{cor} in hours^{-1} *b.* Half-lives in hours *c.* Standard error of the rate constant *d.* Coefficient of determination determined for the least squares fit of the degradation data to a pseudo-first order kinetics model.

Photolysis Experimental Conditions	k_{cor} [a]	$t_{1/2}$ [b]	SE [c]	R^2 [d]
Artificial Solar Irradiation				
18 MΩ-cm Water	0.0088	78.98	0.0017	0.5252
Toolik Early DOM	1.1083	0.63	0.0794	0.8985
Fog 1 DOM	0.7570	0.92	0.0453	0.9332
Fog 1 DOM & FeCl3	1.0682	0.65	0.0489	0.9541
PLFA DOM	1.0859	0.64	0.0718	0.9123
PLFA DOM & FeCl3	1.1866	0.58	0.0550	0.9529
SRFA DOM	1.1169	0.62	0.0891	0.8724
SRFA DOM & FeCl3	1.1816	0.59	0.0508	0.9592
Toolik Late DOM	0.7946	0.87	0.0724	0.8398
Toolik Late DOM & $FeCl_3$	0.9337	0.74	0.0401	0.9594

Table B.3.2. Chlorpyrifos photodegradation pseudo first order rate constants (k_{cor}) and half-lives in units of time, with and without the addition of fulvic acids, under artificial and natural solar irradiation. *a.* k_{cor} in hours^{-1} *b.* Half-lives in hours *c.* Standard error of the rate constant *d.* Coefficient of determination determined for the least squares fit of the degradation data to a pseudo-first order kinetics model.

Photolysis Experimental Conditions	k_{cor} [a]	$t_{1/2}$ [b]	SE [c]	R^2 [d]
Artificial Solar Irradiation				
18 MΩ-cm Water pH 5	0.0392	17.69	0.0021	0.9362
18 MΩ-cm Water pH 7	0.0265	26.17	0.0011	0.9606
18 MΩ-cm Water pH 9	0.0347	19.99	0.0012	0.9717
Fog 1 DOM pH 5	0.0584	11.86	0.0021	0.9739

Table B.3.2. continued

Fog 1 DOM pH 7	0.0445	15.56	0.0020	0.9549
Fog 1 DOM pH 9	0.0552	12.54	0.0022	0.9653
Fog 1 DOM & FeCl3	0.1520	4.56	0.0055	0.9709
Toolik Early DOM pH 5	0.0575	12.06	0.0036	0.9355
Toolik Early DOM pH 7	0.0601	11.52	0.0018	0.985
Toolik Early DOM pH 9	0.0530	13.09	0.0020	0.9686
PLFA DOM pH 5	0.0402	17.23	0.0024	0.9225
PLFA DOM pH 7	0.0528	13.13	0.0014	0.9839
PLFA DOM pH 9	0.0505	13.73	0.0021	0.96
PLFA DOM & FeCl3	0.0739	9.38	0.0091	0.7409
SRFA DOM pH 5	0.0440	15.76	0.0014	0.9767
SRFA DOM pH 7	0.0453	15.30	0.0018	0.9666
SRFA DOM pH 9	0.0489	14.18	0.0017	0.9726
SRFA DOM & FeCl3	0.0640	10.82	0.0029	0.9536
Toolik Late DOM pH 5	0.0453	15.29	0.0022	0.9467
Toolik Late DOM pH 7	0.0439	15.78	0.0022	0.9477
Toolik Late DOM pH 9	0.0435	15.91	0.0017	0.9676
Toolik Late DOM & FeCl3	0.0639	10.84	0.0026	0.9660
Natural Solar Irradiation at 69°N				
Fog 1	0.0050	137.85	0.0006	0.7729
Fog 2	0.0030	233.83	0.0005	0.6828
Toolik Lake	0.0014	503.44	0.0003	0.6422
18 MΩ-cm Water	0.0003	2518.17	0.0003	0.0388

APPENDIX C. DISCUSSION

Table C.4.1. Correlations between chlorothalonil photodegradation rate constants (k_{cor}) in the presence of the various fulvic acid extracts and respective isolate characteristics. *a.* Pearson's correlation r coefficient, degrees of freedom = 3

DOM characteristics	r [a]	P-Value
MDLT	-0.1855	0.7651
CRAM	0.7505	0.1439
Carbohydrates and Peptides	-0.4860	0.4066
Aromatics	0.8365	0.0774
Carbohydrates and Peptides / Aromatics	-0.8563	0.0639
CRAM / Carbohydrates and Peptides	0.5813	0.3039
CRAM / Aromatics	-0.5587	0.3276
MDLT / Aromatics	-0.7997	0.1043
FI	0.1975	0.7502
C/N	-0.2915	0.6342

Table C.4.2. Correlations between chlorothalonil photodegradation rate constants (k_{cor}) in the presence of the various fulvic acid extracts, with the addition of iron, and respective isolate characteristics. *a.* Pearson's correlation r coefficient, degrees of freedom = 2

DOM characteristics	r [a]	P-Value
MDLT	0.0293	0.9707
CRAM	0.9389	0.0611
Carbohydrates and Peptides	-0.3999	0.6001
Aromatics	0.9335	0.0665
Carbohydrates and Peptides / Aromatics	-0.9533	0.0467
CRAM / Carbohydrates and Peptides	0.6323	0.3677
CRAM / Aromatics	-0.7241	0.2759
MDLT / Aromatics	-0.7586	0.2414
FI	0.2406	0.7594
C/N	-0.4574	0.5426

Table C.4.3. Correlations between chlorpyrifos photodegradation rate constants (k_{cor}) in the presence of the various fulvic acid extracts and respective isolate characteristics. *a.* Pearson's correlation r coefficient, degrees of freedom = 3

DOM characteristics	r[a]	P-Value
MDLT	0.4755	0.4182
CRAM	0.1810	0.7709
Carbohydrates and Peptides	-0.6027	0.2820
Aromatics	0.5344	0.3536
Carbohydrates and Peptides / Aromatics	-0.6979	0.1901
CRAM / Carbohydrates and Peptides	0.4307	0.4691
CRAM / Aromatics	-0.5487	0.3383
MDLT / Aromatics	-0.2583	0.6749
FI	0.5962	0.2886
C/N	-0.3473	0.5669

Table C.4.4. Correlations between chlorpyrifos photodegradation rate constants (k_{cor}) in the presence of the various fulvic acid extracts, with the addition of iron, and respective isolate characteristics. *a.* Pearson's correlation r coefficient, degrees of freedom = 2

DOM characteristics	r[a]	P-Value
MDLT	0.5708	0.4292
CRAM	-0.2433	0.7567
Carbohydrates and Peptides	0.2931	0.7069
Aromatics	0.0035	0.9965
Carbohydrates and Peptides / Aromatics	0.0676	0.9324
CRAM / Carbohydrates and Peptides	-0.2690	0.7311
CRAM / Aromatics	-0.3468	0.6532
MDLT / Aromatics	0.2019	0.7981
FI	0.0566	0.9434
C/N	0.0469	0.9531